BMC Plant Biology

RESEARCH Open Access

Genome-wide analysis of miR172-mediated response to heavy metal stress in chickpea (*Cicer arietinum* L.): physiological, biochemical, and molecular insights

Sumeyra Ucar[1], Esra Yaprak[1], Esma Yigider[2*], Ayse Gul Kasapoglu[1], Burak Muhammed Oner[1], Emre Ilhan[1], Abdulkadir Ciltas[2], Ertan Yildirim[3] and Murat Aydin[2*]

Abstract

Background Chickpea (*Cicer arietinum* L.), a critical diploid legume in the Fabaceae family, is a rich source of protein, vitamins, and minerals. However, heavy metal toxicity severely affects its growth, yield, and quality. MicroRNAs (miRNAs) play a crucial role in regulating plant responses to both abiotic and biotic stress, including heavy metal exposure, by suppressing the expression of target genes. Plants respond to heavy metal stress through miRNA-mediated regulatory mechanisms at multiple physiological, biochemical, and molecular levels. Although the Fabaceae family is well represented in miRNA studies, chickpeas have been notably underrepresented. This study aimed to investigate the effects of heavy metal-induced stress, particularly from 100 µM concentrations of cadmium (Cd), chromium (Cr), nickel (Ni), lead (Pb), and 30 µM arsenic (As), on two chickpea varieties: ILC 482 (sensitive) and Azkan (tolerant). The assessment focused on physiological, biochemical, and molecular parameters. Furthermore, a systematic characterization of the miR172 gene family in the chickpea genome was conducted to better understand the plant's molecular response to heavy metal stress.

Results Variance analysis indicated significant effects of genotype (G), treatment (T), and genotype-by-treatment (GxT) interactions on plant growth, physiological, and biochemical parameters. Heavy metal stress negatively impacted plant growth in chickpea genotypes ILC 482 and Azkan. A reduction in chlorophyll content and relative leaf water content was observed, along with increased cell membrane damage. In ILC 482, the highest hydrogen peroxide (H_2O_2) levels in shoot tissue were recorded under As, Cd, and Ni treatments, while in Azkan, peak levels were observed with Pb treatment. Malondialdehyde (MDA) levels in root tissue were highest in ILC 482 under Cd and Ni exposure and in Azkan under As, Cr, and Cd treatments. Antioxidant enzyme activities, including superoxide dismutase (SOD), catalase (CAT), peroxidase (POD), and ascorbate peroxidase (APX), were significantly elevated under heavy metal stress in both genotypes. Gene expression analysis revealed upregulation of essential antioxidant enzyme genes,

*Correspondence:
Esma Yigider
esma.yigider@atauni.edu.tr
Murat Aydin
maydin@atauni.edu.tr

Full list of author information is available at the end of the article

such as *SOD*, *CAT*, and *APX*, with *APX* showing notable increases in both shoot and root tissues compared to the control. Additionally, seven miR172 genes (*miR172a*, *miR172b*, *miR172c*, *miR172d*, *miR172e*, *miR172f*, and *miR172g*) were identified in the chickpea genome, distributed across five chromosomes. All genes exhibited conserved hairpin structures essential for miRNA functionality. Phylogenetic analysis grouped these *miR172* genes into three clades, suggesting strong evolutionary conservation with other plant species. The expression analysis of *miR172* and its target genes under heavy metal stress showed varied expression patterns, indicating their role in enhancing heavy metal tolerance in chickpea.

Conclusions Heavy metal stress significantly impaired plant growth and physiological and biochemical parameters in chickpea genotypes, except for cell membrane damage. The findings underscore the critical role of miR172 and its target genes in modulating chickpea's response to heavy metal stress. These insights provide a foundational understanding for developing stress-tolerant chickpea varieties through miRNA-based genetic engineering approaches.

Keywords Antioxidant enzyme, AP2, Genome-wide analysis, LMBR1, Oxidative stress

Background

The world population is expected to reach 9.7 billion by 2050, necessitating increased food production, particularly cereals and grain legumes [1]. Moreover, there is a progressive rise in the inclination toward plant-based proteins, as evidenced by the current surge in demand for pulses [2]. Common vegetable protein sources include oilseeds, grains, and legumes cultivated commercially [3]. Chickpea (*Cicer arietinum* L.) is a major leguminous crop with a high concentration of carbs, starch, protein, crude fiber, vitamins, and minerals [4]. Chickpea also plays a crucial role in agriculture by facilitating the binding of free nitrogen in the air to the soil through a symbiotic relationship with Rhizobium bacteria [5]. Based on 2020 FAO data, India, Australia, Turkey, and Ethiopia, are among the top five countries in chickpea production, producing the most chickpeas for global markets with about 15.7 million tons [6]. However, the collective efficiency of chickpea production has significantly decreased in recent years because of escalating levels of heavy metals in the soil [7, 8].

In recent years, anthropogenic activities, rapid urbanization, and increased industrial activities to meet the growing population's needs have led to heavy metal accumulation because of environmental pollution [9, 10]. Furthermore, by promoting their mobility and intensifying their hazardous effects, climate change's direct influence may aid in releasing heavy metals from the structure of organic substances [11]. The toxicity of heavy metals is determined by their bioavailability, dosage, density, and mobility [12–14]. Density limits range from 3.5 g/cm3 to 7 g/cm^3 [15]. Elements with a density of more than 5 g/cm^3 can be categorized as non-essential and less/extremely toxic to plant growth and development [16–18]. The presence of toxic heavy metals such as arsenic [(As), density: 5.72 g/cm^3], cadmium [(Cd), density: 8.65 g/cm3], chromium [(Cr), density: 7.2 g/cm^3, nickel [(Ni), density: 8.90 g/cm^3] and lead [(Pb), density: 11.35 g/cm^3] in soil has become a significant environmental issue, posing high toxicity to living organisms [19–23]. Even low concentrations of heavy metals such as As, Cd, Pb, and mercury (Hg) disrupt biochemical and physiological processes in the plant and reduce productivity [24, 25]. Heavy metal stress negatively affects many essential enzymes for plant metabolism, resulting in the denaturation of proteins, loss of membrane integrity, decreased photosynthesis and respiration, and an imbalance of reactive oxygen species (ROS) such as superoxide radicals ($O_2^{\bullet-}$), hydrogen peroxide (H_2O_2), hydroxyl radical ($HO^{\bullet}$) singlet oxygen ($^1O_2$), and alkoxyl ($RO^{\bullet}$) and peroxyl ($ROO^{\bullet}$) radical [26, 27]. These extreme accumulations of ROSs have a role in causing oxidative damage by harming lipids in cell membranes and essential biomolecules such as nucleic acids, carbohydrates, proteins, and lipids, eventually triggering cell death [28–31].

Several studies have shown that metal toxicity changes the amount of chlorophyll in leaves, decouple photosynthetic enzymes, slows down growth and biomass, changes protein structure, changes cell redox state, and lowers antioxidant enzyme activity [32–37]. Plant antioxidative defense uses enzymatic and non-enzymatic components to scavenge or suppress ROS to prevent/delay cellular damage [38]. The antioxidant system of defense is composed of two groups: (i) enzymatic antioxidants, including superoxide dismutase (SOD), catalase (CAT), ascorbate peroxidase (APX), and peroxiredoxin (Prx), etc. (ii) non-enzymatic antioxidants such as vitamins [ascorbic acid (AA) and α-tocopherol], reduced glutathione (GSH), carotenoids, flavonoids and proline [39–41].

Plants perceive signals from their severe climate environment, regulate many signal-transduction processes, and direct and initiate their stress regulatory pathways to respond to stress [42]. These stress response regulatory mechanisms include physiological, biochemical (i.e. enzymatic antioxidants and amino acids), and molecular mechanisms. All signaling pathways have the potential

to activate specific transcription factors (TFs), which in turn facilitate the transcription of essential genes responsible for maintaining plant homeostasis during periods of stress [43]. TFs are key regulators of gene expression that can simultaneously regulate many genes and play a role in the response to abiotic stress [44]. Plant-conserved mature microRNAs (miRNAs) are 20–25 nt long and generated from stem-loop sections of about 70 nt RNA precursors by RNase III Dicer-like enzymes [45, 46]. Various plant species have documented over 7,000 mature miRNAs and over 6,000 precursor miRNAs up to this present [47]. These molecules facilitate post-transcriptional silencing by binding to specific locations in the 3′ UTR region of the target messenger RNA (mRNA), leading to degradation or inhibition of mRNA translation [48]. Recent research on miRNAs and their targets has shown that plants have significant regulatory functions, particularly in adapting to different stressors, promoting plant growth and development, regulating gene interactions, and responding to hormonal changes [49–51].

Table 1 The variance analysis results of the parameters[1]

Parameters	Sources of variation (Mean square)			
	Genotype (G) (df = 1)	Treatment (T) (df = 5)	G x T (df = 5)	Error (df = 36)
SL (cm)	26.255**	12.280**	15.330**	0.196
RL (cm)	31.687**	77.313**	3.225**	0.486
CMD (%)	2.154^{ns}	264.768**	23.005**	0.756
RWC (%)	33.413**	391.208**	91.922**	0.682
CC (SPAD)	8.841**	62.667**	120.458**	0.060
S-H_2O_2 (µmol/g)	7840.109**	32571.190**	14355.340**	109.038
R-H_2O_2 (µmol/g)	159.547^{ns}	33539.944**	5560.888**	202.365
S-MDA (µmol/g)	0.283**	0.434**	0.267**	0.001
R-MDA (µmol/g)	0.731**	1.091**	0.261**	0.001
S-SOD (EU/g)	0.232*	2.212**	0.435**	0.035
R-SOD (EU/g)	0.301**	0.964**	0.929**	0.017
S-CAT	0.116**	0.312**	0.024**	0.00011
R-CAT	0.016**	0.194**	0.098**	0.0012
S-POD (EU/g)	271.395**	39.773**	25.099**	0.019
R- POD (EU/g)	167.626**	85.049**	29.842**	0.005
S-APX (EU/g)	0.528**	0.377**	0.125**	0.00003461
R- APX (EU/g)	0.009**	0.277**	0.071**	0.00004168
S-Proline (µmol/g)	0.065**	0.024**	0.033**	0.000
R-Proline (µmol/g FW)	0.031**	0.065**	0.032**	0.000

[1]SL Shoot length, RL Root length, CMD Cell membrane damage, RWC Relative water content, CC chlorophyll content, S Shoot, R Root, H_2O_2 Hydrogen peroxide, MDA Malondialdehyde, SOD Superoxide dismutase, CAT Catalase, POD Peroxidase, and APX; Ascorbate peroxidase

*. **: significant at 0.05 and 0.01 level. respectively. ^{ns}: non-significant at 0.05 level

miR172 is a conserved short non-protein-coding RNA molecule with 21 nt responsible for regulating diverse plant developmental processes and gene regulation [52]. miR172 is one of the earliest miRNA families in the kingdom of plants, having been found first in Arabidopsis by the cloning and sequencing of short RNAs [53]. There are three isoforms of miR172 in Arabidopsis encoded by the genes *mir172a/b*, *c/d*, and *e* [54]. The miR172 targets the mRNAs of the APETALA2-LIKE (AP2-LIKE) TF family, and this interactive relation is conserved in all spermatophytes [55]. The *miR172* gene family regulates meristem length, root elongation, trichome initiation, shoot branching, and flower competence [56]. Many studies show that miR172 is essential for plant growth and response to environmental stress such as salinity, drought, heat, and heavy metals [57–59].

No study has explored the effects of As, Cd, Cr, Ni, and Pb on miR172 expression in chickpeas. This study examined chickpeas' physiological, morphological, and molecular responses to five heavy metal stresses. Moreover, the *miR172* gene family was identified, and chromosomal locations, 2D structures, motifs, and phylogenetic relationships were investigated.

Results

Growth parameters

SL and RL varied significantly by G and treatment T (Table 1). The observed GxT interaction effect for both SL and RL indicates a significant variation in the impact of heavy metals across different genotypes. Both genotypes (ILC 482 and Azkan) exhibited notable treatment-specific disparities in SL and RL compared to the control group in this study. The Azkan genotype showed the most significant reduction in shoot length in the As treatment group, while the ILC 482 genotype showed a significant shortening in the Cd treatment. The SL of the Ni-treated groups was more significant than that of the control group in both genotypes (Fig. S1A). Both genotypes exhibited a substantially decrease in RL when exposed to heavy metals compared to the control group. Moreover, both genotypes exhibited the lowest average RL when subjected to Cr and Cd treatments, as compared to other metal treatments (Fig. S1B).

Cell membrane damage (CMD)

According to the variance analysis results, the effect of genotype (G) on CMD was insignificant ($p > 0.05$), while the effect of treatment (T) and GxT interaction was very significant ($p < 0.01$) (Table 1). The results indicated that all heavy metal treatments significantly increased CMD levels compared to the control group in both genotypes. Notably, As treatment resulted in the highest CMD levels in both genotypes, while Cd treatment had relatively lower impacts, however, all metals showed statistically

significant detrimental effects compared to the control ($p<0.001$) (Fig. S2).

Relative water content (RWC)

Genotypes and treatments considerably impacted RWC. The observed interaction between genotype and treatment can be attributed to the variability in the RWC of different genotypes (Table 1). Heavy metal application resulted in a reduction in RWC in both genotypes compared to the control. Among all the metal treatments, the Ni and Pb treatments exhibited the most significant decrease in RWC in the ILC 482 genotype. On the other hand, in the Azkan genotype, Cr treatment was shown to be the heavy metal that caused the most significant reduction in RWC (Fig. S3).

Chlorophyll content (CC) (SPAD)

On chlorophyll content, the effect of genotype (G), treatment (T), and their interaction (GxT) was very significant ($p<0.01$) (Table 1). The ILC 482 genotype exhibited a reduction in CC across all heavy metal treatments compared to the control. Among these treatments, Cd and Cr caused the most minor reductions, while Ni, Pb, and As treatments exhibited the lowest CC levels (Fig. S4). The chlorophyll content of the Azkan genotype varied according to the treatment. This genotype showed a significant increase in CC content in Ni, Cd, and As treatments compared to the control. At the same time, a decrease was determined in Cr and Pb treatments (Fig. S4).

Oxidative stress indicators

H_2O_2 and MDA levels were significantly affected by the treatments (Table 1). In both tissue types of both genotypes, the amount of H_2O_2 increased in heavy metal treatments compared to the control (Fig. S5). The Azkan genotype showed the maximum quantity of H_2O_2 in shoot tissue when treated with Pb, while the ILC 482 genotype showed the highest amounts in treatments with As, Cd, and Ni, respectively (Fig. S5A). For the ILC 482 genotype, the As treatment had the most significant quantity of H_2O_2 in the root tissue; for the Azkan genotype, the As, Cd, and Cr treatments had the highest amount (Fig. S5B). Moreover, both genotypes demonstrated a rise in MDA content in heavy metal treatments relative to the control, which is consistent with the results shown in H_2O_2. The ILC 482 genotype showed the greatest MDA level in shoot tissue regarding Cd and Cr treatments, whereas the Azkan genotype showed the highest MDA content in As and Cd treatments (Fig. S5C). When subjected to Cd and Ni treatments, the ILC 482 genotype exhibited the highest MDA concentration in root tissue. In contrast, the Azkan genotype showed the highest MDA concentration when treated with As, Cr, and Cd (Fig. S5D).

Antioxidant enzymes

The activities of SOD, CAT, POD, and APX enzymes were significantly affected by both genotype and treatment. Moreover, the fact that the activities of these enzymes in genotypes differed according to the treatments caused the GxT interaction to be significant (Table 1). Both genotypes showed an increase in SOD, POD, and APX in both shoot and root tissues under heavy metal treatments compared to the control. The most significant levels of SOD in shoot tissue of the genotypes were noticed in the Pb treatment for the ILC 482 genotype and the As and Cd treatments for the Azkan genotype (Fig. S6A). It was most remarkable in root tissue in the Ni and As treatments for the ILC 482 genotype and the As treatment for the Azkan genotype (Fig. S6B). The CAT enzyme activities for both genotypes (ILC-482 and Askan) show a significant increase in response to heavy metal treatments compared to control conditions in both tissues. Notably, the shoot tissue of the ILC 482 genotype exhibited the highest CAT activity following Cd and Cr treatments (Fig. 6SC). Similarly, in the Azkan genotype, Cd and Ni treatments resulted in a remarkable rise in CAT activity. In the root tissue, the ILC 482 genotype displayed the highest CAT activity in response to Cd, Pb, and As treatments, while in the Azkan genotype, the highest activity was observed following As treatments (Fig. S6D). The highest levels of POD activity were observed in shoot tissue treated with Pb in the ILC 482 genotype and As in the Azkan genotype (Fig. S6E). Root tissue exhibited the most significant levels of POD activity in all metal treatments, excluding Cd in the ILC 482 genotype and As in the Azkan genotype (Fig. S6F). Furthermore, after assessing the APX levels in the shoot and root tissues of the genotypes, it was found that the ILC 482 genotype exhibited the greatest APX concentration in both tissues under the As treatment. The Azkan genotype exhibited the greatest APX value in the shoot tissue when exposed to Ni and in the root tissue when treated with CR application (Fig. S6G and H).

Proline

The statistical analysis revealed a considerable change in proline content, which serves as a stress indicator, among different genotypes and treatments. In addition, the differences in proline content among different genotypes in the treatments resulted in significant GxT interaction (Table 1). Both genotypes exhibited a rise in proline content in reaction to heavy metal stress, with the same treatments resulting in a more notable increase than others. The genotype ILC 482 exhibited the maximum proline content in both tissues with Ni treatment and in the Azkan genotype under Cr treatment (Fig. S7A and B). Both genotypes had the lowest proline content in the

control plants, suggesting that the metal treatments had a stress-inducing impact.

Correlation and PCA analysis

The length of the roots and shoots of plants and the RWC and CMD showed a negative correlation with the levels of MDA and H_2O_2. CC showed a positive relationship with MDA. In addition, H_2O_2 content exhibited a positive correlation with SOD, CAT, POD, and APX contents. Moreover, the proline content had a positive correlation with MDA, H_2O_2, SOD, CAT, POD, and APX contents (Fig. 1).

PCA was conducted in the study to comprehend the fundamental structure of the dataset, which encompasses a range of biochemical and physiological indicators. Four principal components with Eigen values greater than one were identified, cumulatively explaining 97.24% of the total variance observed in the data (Table 2). PC1 accounted for 65.05% of the total variance, making it the most important contributor. The high negative loadings for several parameters, including CMD, MDA, H_2O_2, SOD, CAT, POD, and APX in both shoots and roots, suggest that PC1 primarily captures oxidative stress responses and antioxidant enzyme activities. This component likely reflects the intensity of oxidative damage and the plant's antioxidative defense mechanisms. On the other hand, RWC showed a significant positive loading (0.945) on PC1, suggesting a contrasting pattern with oxidative stress indicators. CMD, one of the physiological characters with the highest negative charge, may be used as a heavy metal stress indicator. PC2 explained 13.85% of the variance. It exhibited positive loadings for CAT activity in shoots and root proline content, indicating a correlation between antioxidant activity and osmotic stress adaptation. The significant loadings suggest that PC2 represents the plant's protective and adaptive responses under stress conditions, particularly involving osmolyte accumulation and specific enzymatic activity.

According to biplot analysis, furthermore, the PCA biplot showed clear distinctions between the treatments,

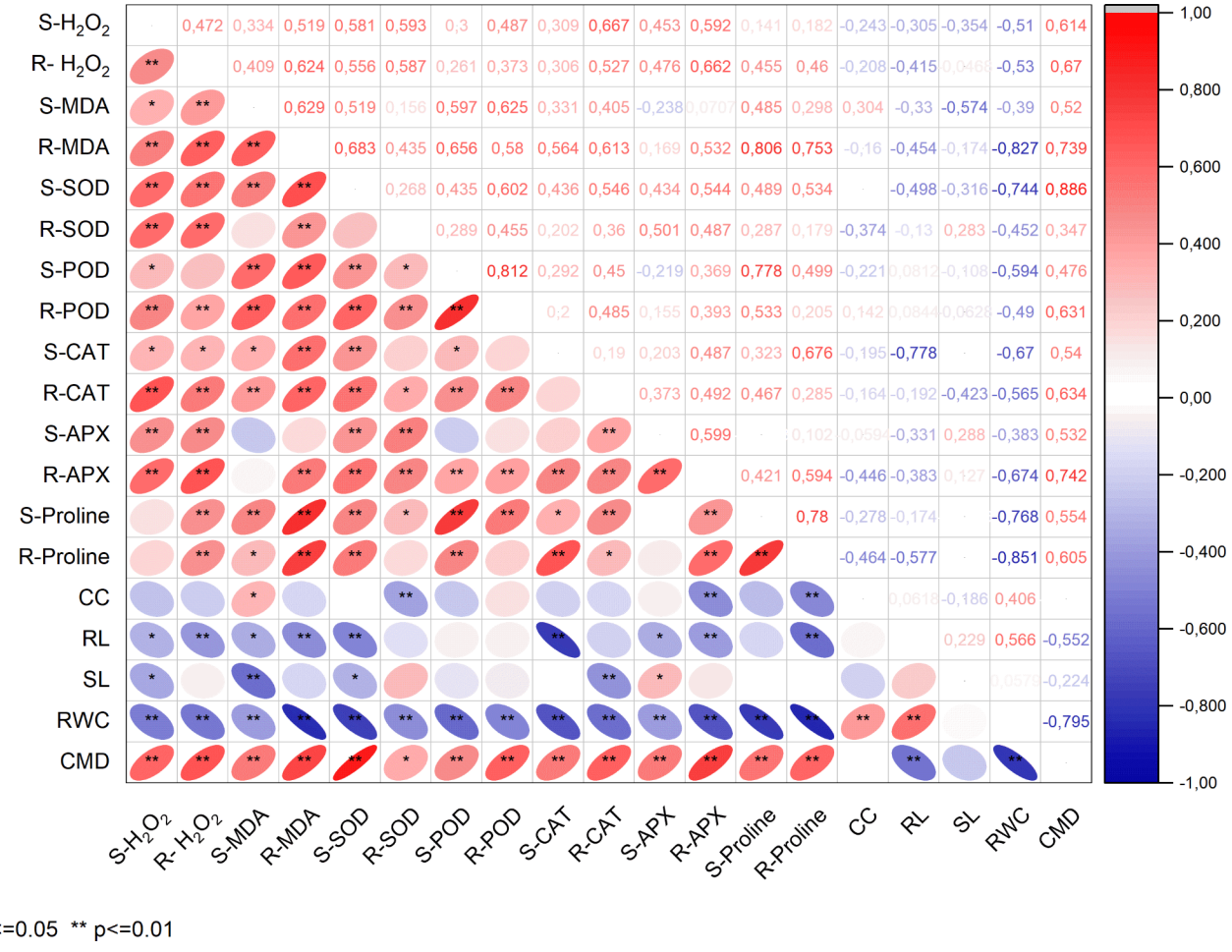

Fig. 1 Heatmap of Pearson's correlation for different parameters of chickpea under heavy metal stress. Red indicates a positive correlation, with darker shades representing stronger correlations. Blue indicates a negative correlation, with darker shades representing stronger negative correlations. Asterisks (*) denote statistically significant correlations, with one asterisk indicating a p-value ≤ 0.05 and two indicating a p-value ≤ 0.01

Table 2 Factor loadings of parameters based on principal components[1]

Variable	PC1	PC2	PC3	PC4
S-H_2O_2	-0.898	-0.249	-0.022	-0.133
R-H_2O_2	-0.850	0.022	0.431	0.160
S-MDA	-0.700	0.377	0.593	0.123
R-MDA	-0.915	0.149	0.133	0.283
S-SOD	-0.993	0.033	0.009	-0.048
R-SOD	-0.826	-0.499	-0.013	0.227
S-CAT	-0.635	0.610	-0.428	0.067
R-CAT	-0.856	-0.389	0.304	-0.104
S-POD	-0.854	-0.226	0.067	-0.455
R- POD	-0.847	-0.517	0.104	-0.067
S-APX	-0.729	-0.486	-0.367	0.312
R- APX	-0.869	-0.112	-0.335	-0.077
S-Proline	-0.952	0.026	0.100	0.101
R-Proline	-0.778	0.553	-0.276	-0.014
CC	0.305	-0.072	0.370	0.874
RL	0.615	-0.721	0.209	-0.240
SL	0.311	-0.464	-0.721	0.402
RWC	0.945	-0.135	0.287	0.038
CMD	-0.995	0.021	-0.050	0.026
Eigenvalue	12.36	2.63	1.96	1.51
Proportion of variance (%)	65.05	13.85	10.34	8.00
Cumulative proportion of variance (%)	65.05	78.91	89.24	97.24

[1] H_2O_2; Hydrogen peroxide, MDA; Malondialdehyde, SOD; Superoxide dismutase, CAT; Catalase; POD; Peroxidase, APX; Askorbate peroxidase, S; Shoot, R; Root, CC; chlorophyll content, RL; Root length, SL; Shoot length, RWC; Relative water content, and CMD; Cell membrane damage

with heavy metal treatments clustering away from the control group (Fig. 2).

PC1, which is mainly associated with growth-related parameters such as SL, RL, and relative RWC. These parameters are closely linked to the control group (#3), suggesting that plants in the control group exhibited better growth and water retention than those treated with heavy metals. Cd (#2) and Cr (#4) shift towards biochemical parameters like CAT and Proline, suggesting that these heavy metals are associated with oxidative stress responses, as indicated by the increased activity of these stress-related enzymes. Ni (#%5), Pb (#6), and As (#1) are positioned negatively along the PC2 axis, showing a negative correlation with root length and certain antioxidant enzyme activities (Fig. 2).

Expression analysis of *SOD*, *CAT*, and *APX* genes under heavy metal stress

When evaluating the expression profile of the SOD gene in ILC 482 and Azkan genotypes, we found that the mRNA expression of SOD in the shoot tissue of ILC-482 was slightly higher in all heavy metal treatments compared to the control, with significant differences between the control and treatments. The expression level of SOD for Azkan was much higher compared to ILC-482. Significant upregulation is observed under Cd and Ni treatments, particularly under Cd stress, where SOD mRNA expression is maximally induced (Fig. S8A). Furthermore, expression levels of SOD in roots of ILC 482 show a significant increase under all heavy metal treatments, especially in response to Cd, Pb, and As, with moderate increases in Ni and Pb conditions. Azkan exhibits similar trends, with AS and Pb treatments inducing the highest SOD expression in roots. Ni and Cr also had a notable induction (Fig. S8B).

All treatments significantly increased CAT mRNA expression in the shoot tissues of ILC482, with Cd and Cr showing the highest induction. The CAT expression in the shoots of Azkan follows a similar pattern, with highly significant increases in response to all treatments compared to control (Fig. S8C). Moreover, Cd, Cr, Pb, and As treatments strongly induce CAT expression in the roots, with the highest mRNA levels observed under Cd stress. The Ni treatment also showed significant upregulation. CAT mRNA expression in the root of Azkan showed a substantial increase in all the heavy metal treatments except for Cd (Fig. S8D).

APX expression in shoots of ILC 482 was significantly upregulated in all treatments, with Cr and Pb showing the highest induction. Azkan also indicated significant APX induction across all metal treatments, with Ni and Cr causing the most pronounced increases (Fig. S8E). All metal treatments highly upregulated APX in the root tissue of both ILC 482 and Azkan genotypes. The ILC 482 genotype showed the highest expression in the Pb application, while the Azkan genotype showed it in the As application (Fig. S8F).

Identification, chromosomal localization, secondary structure characterization of *miR172* family genes in chickpea

Seven *car-miR172* genes, namely *as car-miR172a*, *car-miR172b*, *car-miR172c*, *car-miR172d*, *car-miR172e*, *car-miR172f*, and *car-miR172g*, were identified in *C. arietenium* genome. Table 3 provides the mature sequence, chromosome information, and the start and end positions of the *miR172* gene family members. The lengths of the mature sequences of the *miR172* gene family were 21 nt. The car-miR172 family members were identified on five different chromosomes based on chromosomal localization data (Tables 3 and Fig. 3). The RNAfold web server was used to study and show the secondary structures of the members of the *car-miR172* gene family. Upon examination, it was revealed that all genes had the hairpin structure necessary for miRNA production. All car-miRNAs were in the 3' arm of the secondary stem-loop hairpin structure (Fig. 4).

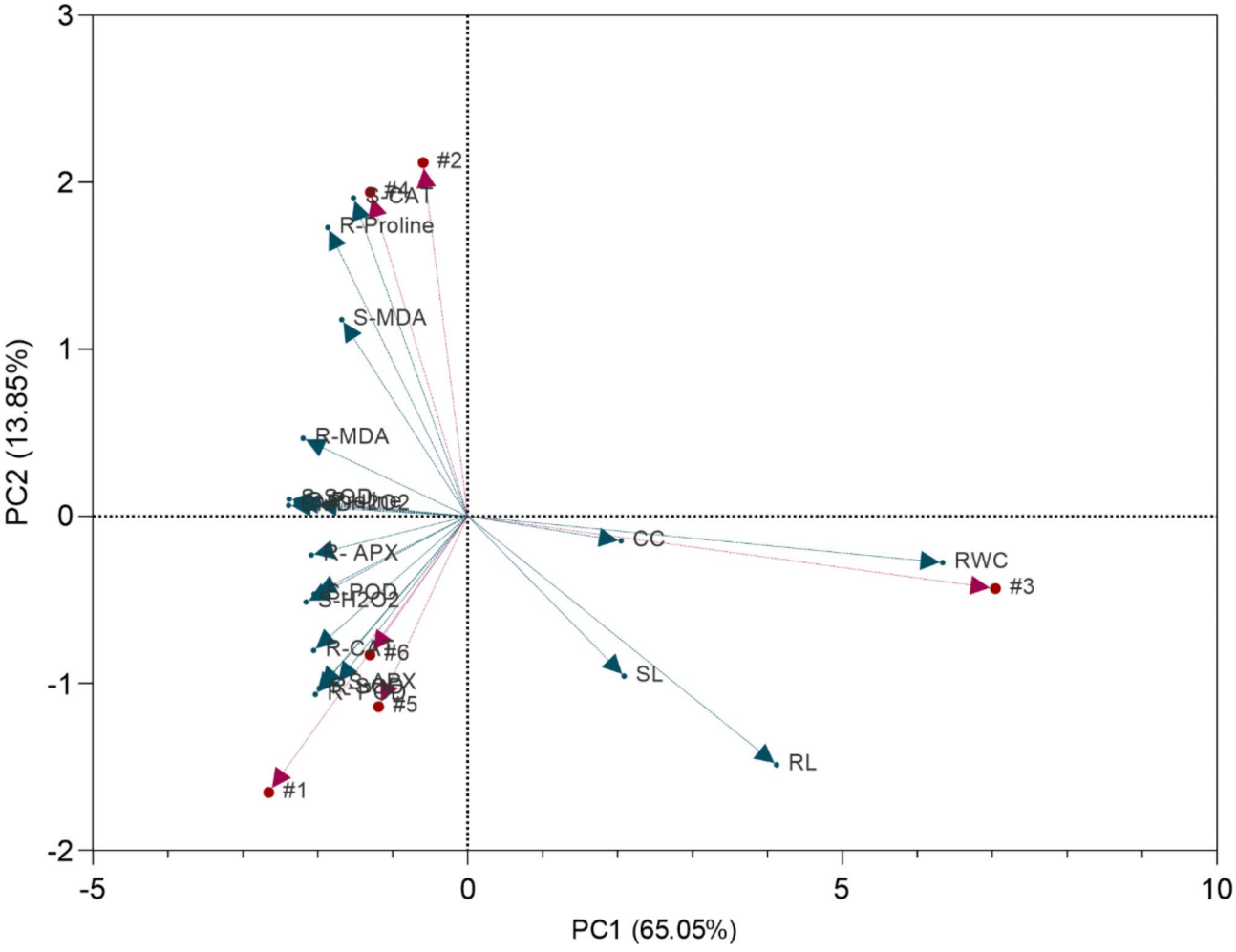

Fig. 2 Principal component analysis for parameters and treatments. #1 As, #2 Cd, #3 Control, #4 Cr, #5 Ni and #6 Pb. SL; Shoot length, RL; Root length, RWC; Relative water content, CMD; Cell membrane damage, CC; chlorophyll content, S; Shoot, R; Root, H_2O_2; Hydrogen peroxide, MDA; Malondialdehyde, SOD; Superoxide dismutase, POD; Peroxidase, and APX; Ascorbate peroxidase

Table 3 Mature sequence, sequence length, and chromosomal localization of Car-miR172 family members

car Gene name	Mature sequence (5′-3′)	Sequence length (nt)	Chromosom No	Starting position	End position
car-miR172a	AGAAUCUUGAUGAUGCUGCAG	21	C11160018	551	663
car-miR172b	AGAAUCUUGAUGAUGCUGCAG	21	CaChr1	11,265,311	11,265,409
car-miR172c	CGAAUCCUGAUGAUGCUGCAG	21	CaChr1	11,960,694	11,960,824
car-miR172d	AGAAUCUUGAUGAUGCUGCAU	21	CaChr2	29,851,857	29,851,967
car-miR172e	AGAAUCUUGAUGAUGCUGCAU	21	CaChr4	9,946,990	9,947,126
car-miR172f	AGAAUCUUGAUGAUGCUGCAU	21	CaChr6	1,018,471	1,018,583
car-miR172g	AGAAUCUUGAUGAUGCUGCAU	21	CaChr6	28,871,855	28,871,978

Identification of conserved motifs and phylogenetic analysis of the car-miR172 family members

As a result of the conserved region analysis of *car-miR172* gene family members, it was determined that 18 nt were conserved. In Fig. 5, each letter represents a nucleotide (A, G, U, C). The height of each letter at a given position indicates the frequency and conservation of that nucleotide at that position across the miR172 family. The overall height of the stack at each position reflects the level of sequence conservation at that position, with higher stacks indicating more significant conservation. This phylogenetic tree shows the evolutionary relationships of the miR172 family among *Cicer arietinum*, *Arabidopsis thaliana*, *Glycine max*, *Medicago truncatula*, and *Oryza sativa*. The results showed the clustering of three major clades, A, B, and C. When the phylogenetic tree was analyzed, it was found that all *Car-miR172* genes were located in clade C. Moreover, *Osa-miR172a*,

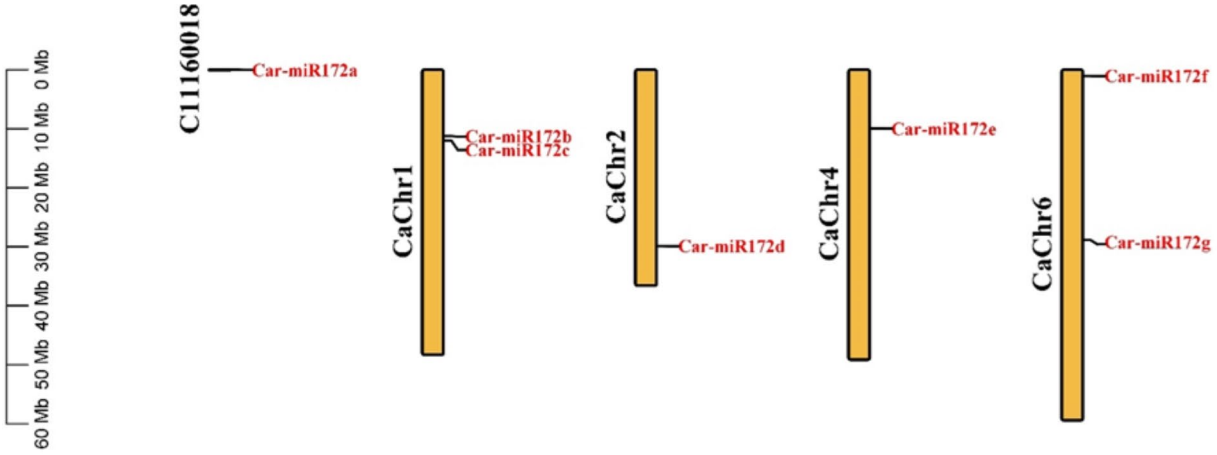

Fig. 3 Chromosomal locations of car-miR172 gene family members. The chromosomes (CaChr1, CaChr2, CaChr4, and CaChr6) are represented as vertical bars, with their length scaled according to Megabase (Mb) pairs indicated on the left

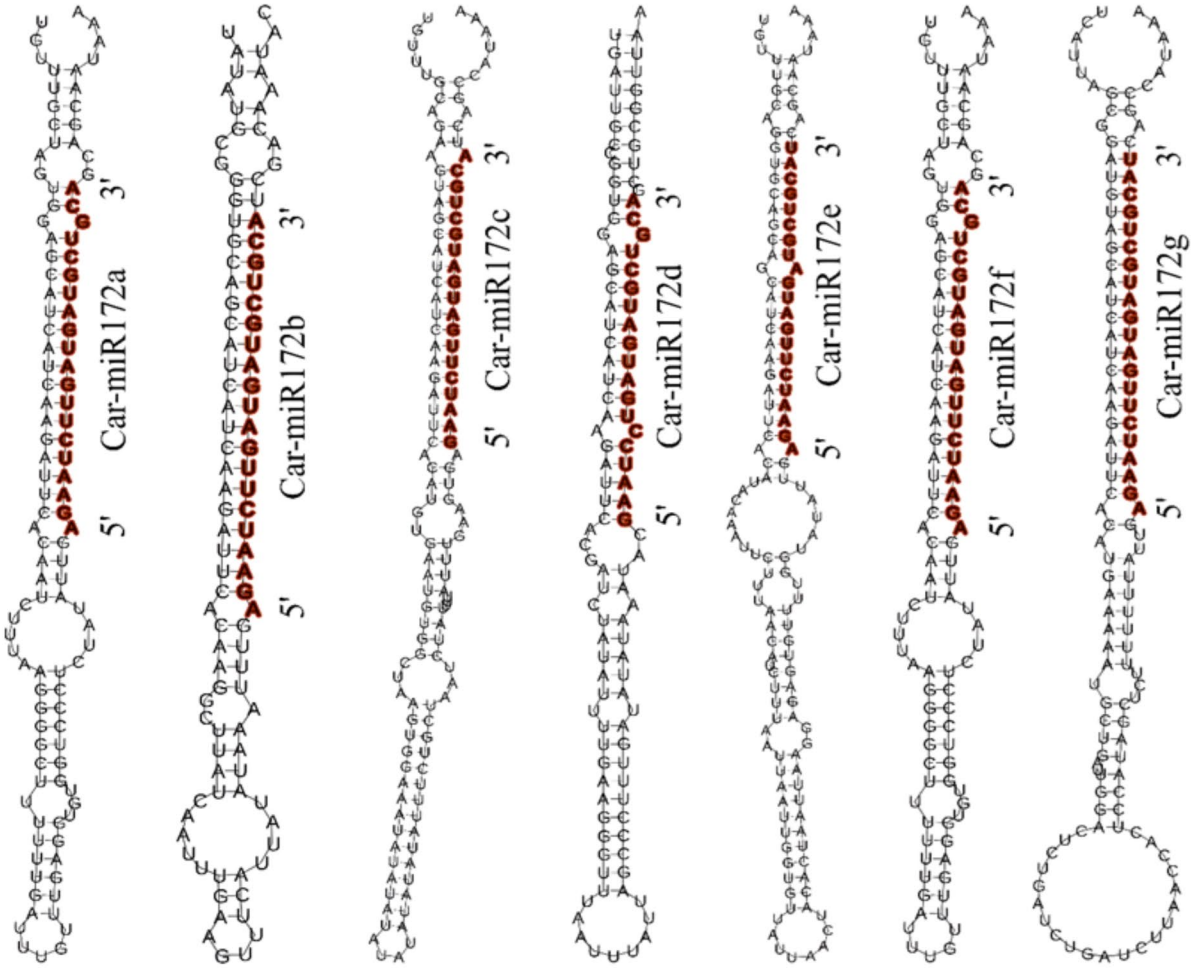

Fig. 4 Stem-loop structures of the *miR172* gene family in Chickpea. Each structure represents the precursor microRNA (pre-miRNA) sequences, with the mature miRNA sequence highlighted in red within the stem region of the hairpin

Fig. 5 The conserved domain analysis results of the mature sequence of the car-miR172 family

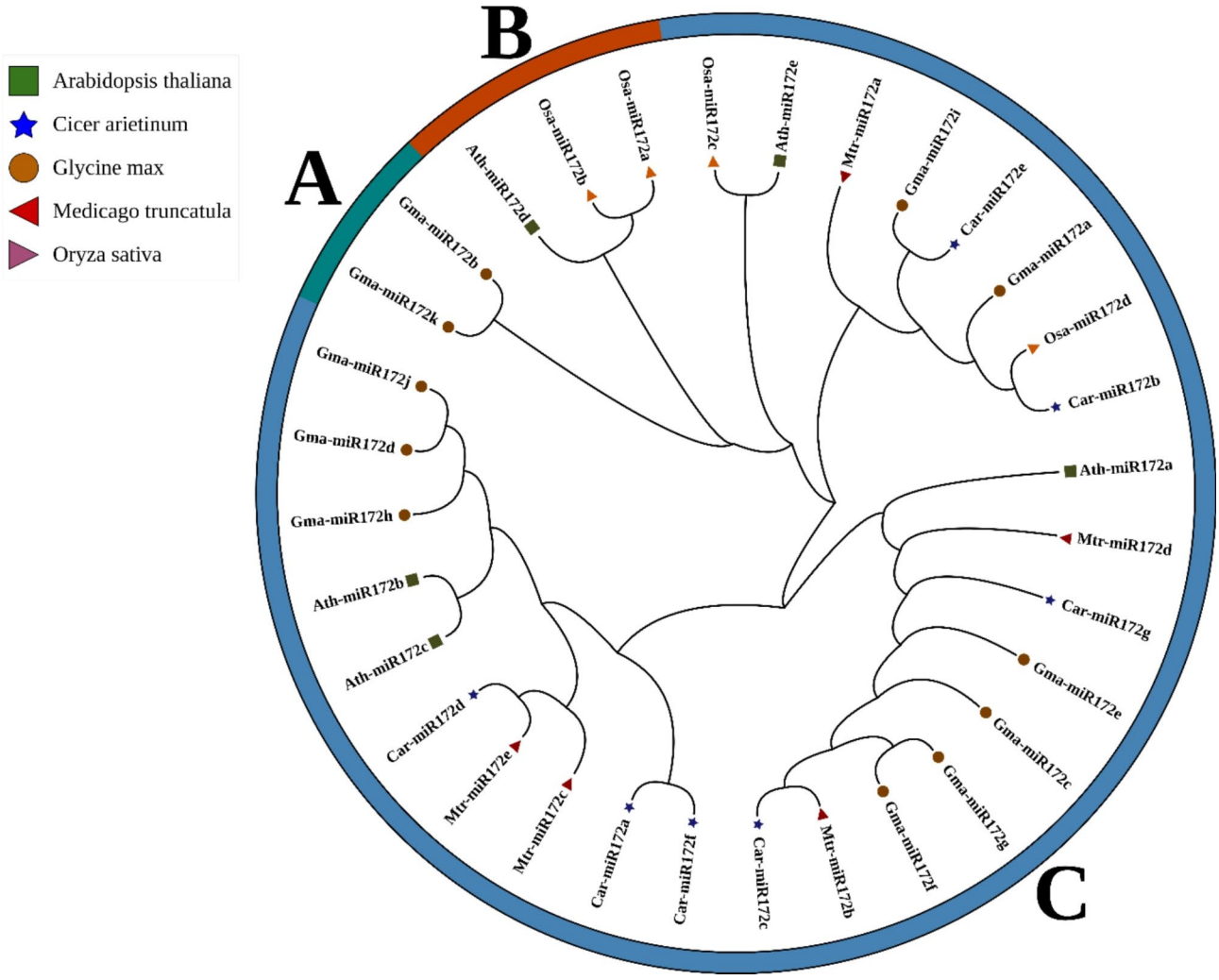

Fig. 6 Evolutionary relationship analysis of the car-miR172 gene family members. The colored symbols on the branches represent the plant species to which each microRNA belongs: Green square: *Arabidopsis thaliana*, Blue star: *Cicer arietinum*, Orange circle: *Glycine max*, Red triangle: *Medicago truncatula*, Brown triangle: *Oryza sativa*

Osa-miR172b, and *Ath-miR172d* genes were located in clade B, while *Gma-miR172b* and *Gma-miR172k* genes were located in clade A. (Fig. 6). These results supported the evolutionary conservation of miR172 family members in chickpea.

Expression analysis of *car-miR172* family members and their target genes under heavy metal stress

The expression status of the *car-miR172* gene family members and its target genes were investigated under five heavy metal stresses in the sensitive genotype (ILC 482) and the resistant genotype (Azkan). The expression

levels of *car-miR172* gene family members and their target genes under heavy metal stress for each genotype are described below.

In the ILC 482 genotype, the expression level of *car-miR172a* was increased in all stresses except for Cd and Ni treatments in the root tissue, whereas an increase was determined only in Ni stress in shoot tissue. *AP2* and *LMBR1* genes in the ILC 482 genotype exhibited a high expression profile under all stresses in both tissues, unlike *car-miR172a*. In the Azkan genotype, the expression of *car-miR172a* increased in shoot tissue in all treatments, while in root tissue, it increased only in the Ni treatment. Again, target genes (*AP2* and *LMBR1*) were increased in both tissue types of the Azkan genotype compared to *car-miR172a* (Fig. 7). *car-miR172b* exhibited an increased expression profile in all stresses in both tissue of both genotypes (Fig. 8). At the same time, the expression levels of Filamentation temperature-sensitive H *(FtsH)*, *AP2*, and Arabidopsis Homolog of Trithorax1 (*ATX1*) genes, which are the target genes of *car-miR172b*, increased (Fig. 8).

The expression level of *car-miR172c* in shoot tissue of genotype ILC 482 increased under Cr and As treatments compared to control, while there was an increase in root tissue, especially Cd and As. While the expression of the *car-miR172c* gene was high in shoots of the Azkan genotype, it was considerably higher in Cr treatment in root tissue. Both genotypes for both tissues show increased gene expression under metal stress conditions *AP2*, *P-type ATPases (P4-ATPase)*, and *V-type ATPases (V-ATPase)*. Moreover, the expression levels vary by gene and treatment, with notable increases in Pb and As across both genotypes and tissues. In terms of these genes, Azkan has higher responses to metal treatments in both shoots and roots, while ILC 482 shows more pronounced expression in Pb and Ni treatments (Fig. 9).

Upon analyzing the expression levels of the *car-miR172d* gene, it was observed that its expression increased in both shoot and root tissues of the ILC 482 genotype across all treatments, except for the Pb treatment in shoot tissue. The expression analysis of the *car-miR172d* gene revealed a significant upregulation in the shoot tissues of the Azkan genotype across all treatments, while one increase was observed in the Cr treatment. The genes *AP2*, *LMBR1*, and *V-ATPase* also exhibited increased expression in both genotypes and tissue types. Notably, the *LMBR1* gene demonstrated the highest level of upregulation among all the genes analyzed (Fig. 10).

In the ILC 482 genotype, the expression of the *car-miR172e* gene increased across all treatments in both shoot and root tissues, except the As treatment in shoot tissue. In contrast, the Azkan genotype exhibited an elevated expression level of the *miR172e* gene in shoot tissue under all heavy metal treatments, while in root tissue, a significant increase was observed only under Cr treatment. Under metal stress conditions, both genotypes

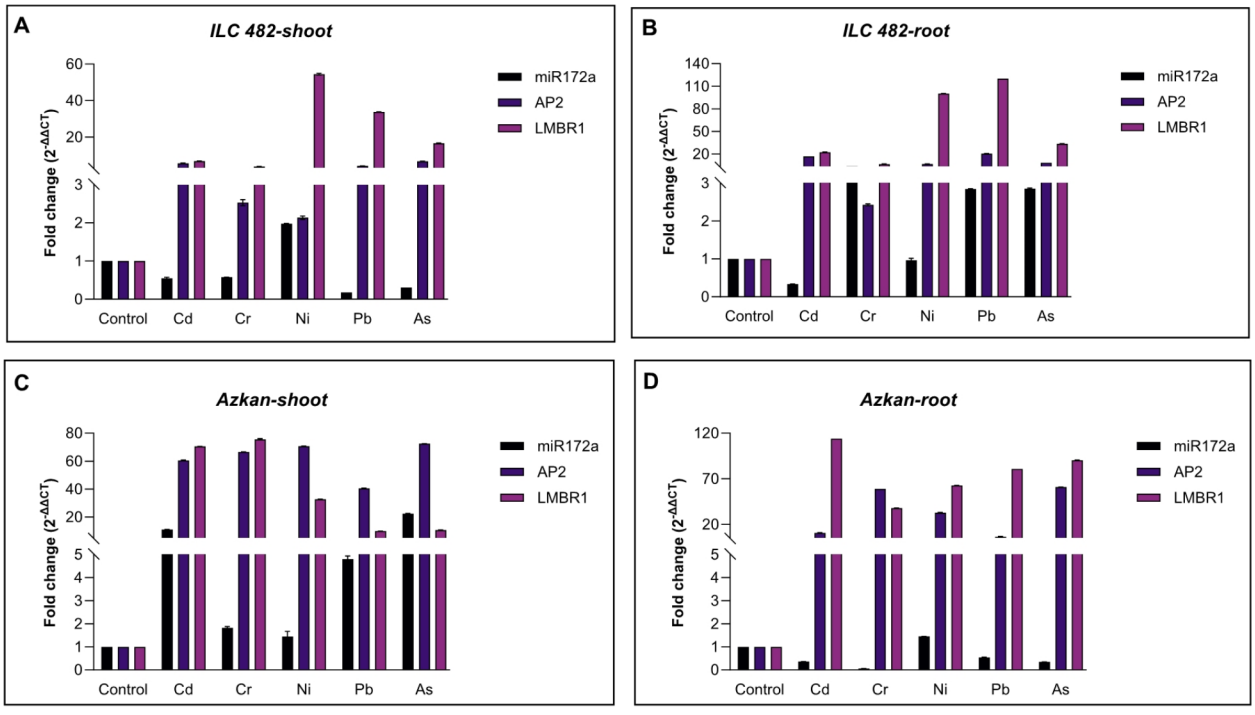

Fig. 7 Expression patterns of *car-miR172a* and its target genes under heavy metal stress. The bars are presented as mean ± SE ($n = 4$)

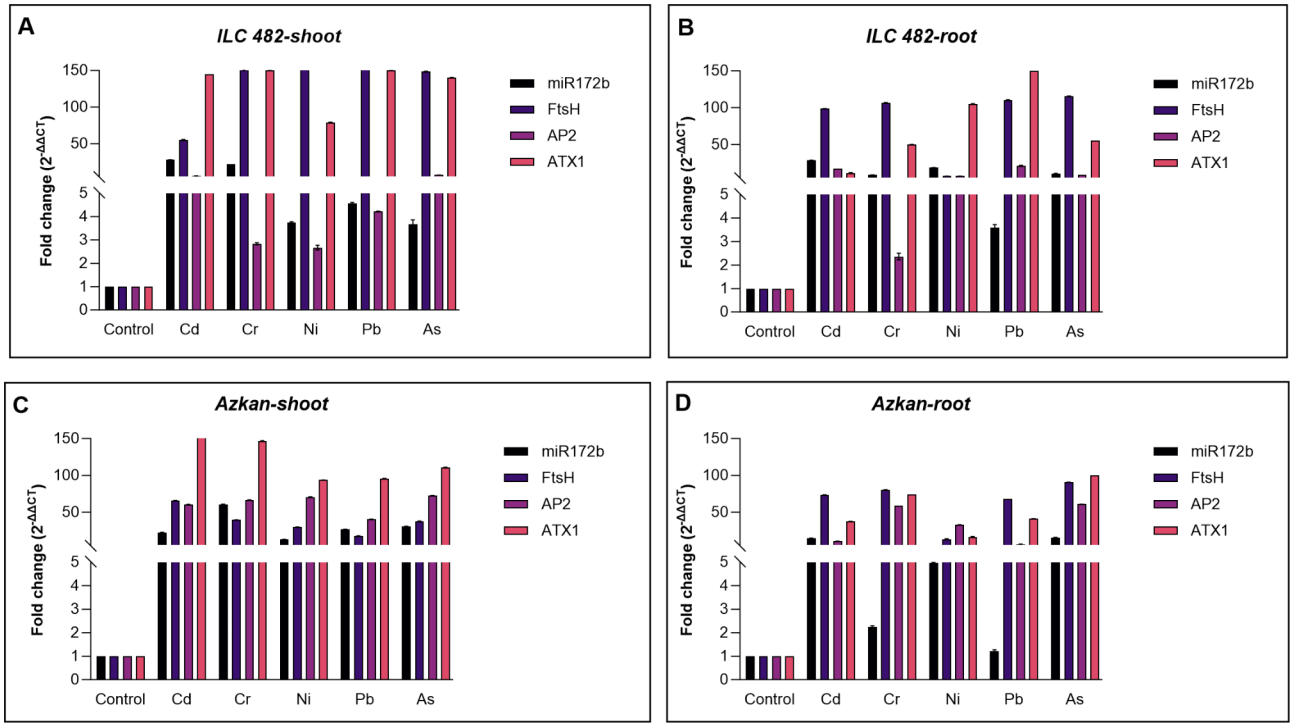

Fig. 8 Expression patterns of *car-miR172b* and its target genes under heavy metal stress. The bars are presented as mean ± SE ($n = 4$)

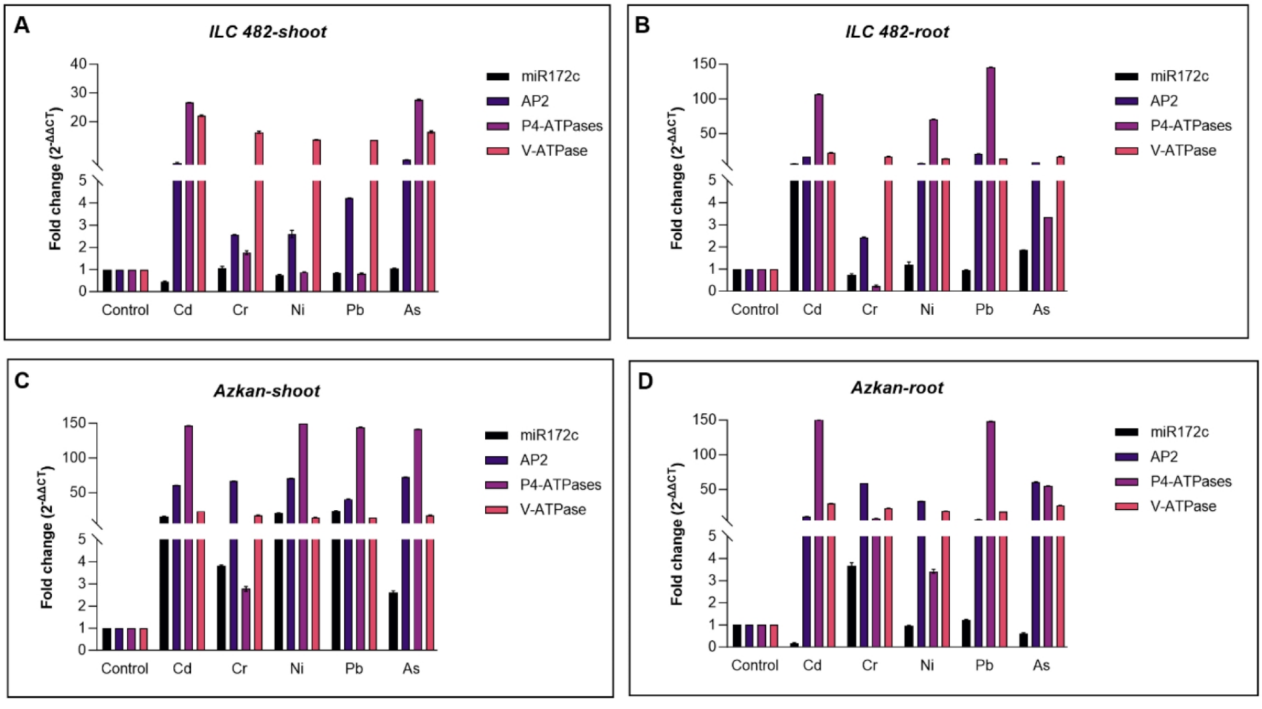

Fig. 9 Expression patterns of *car-miR172c* and its target genes under heavy metal stress. The bars are presented as mean ± SE ($n = 4$)

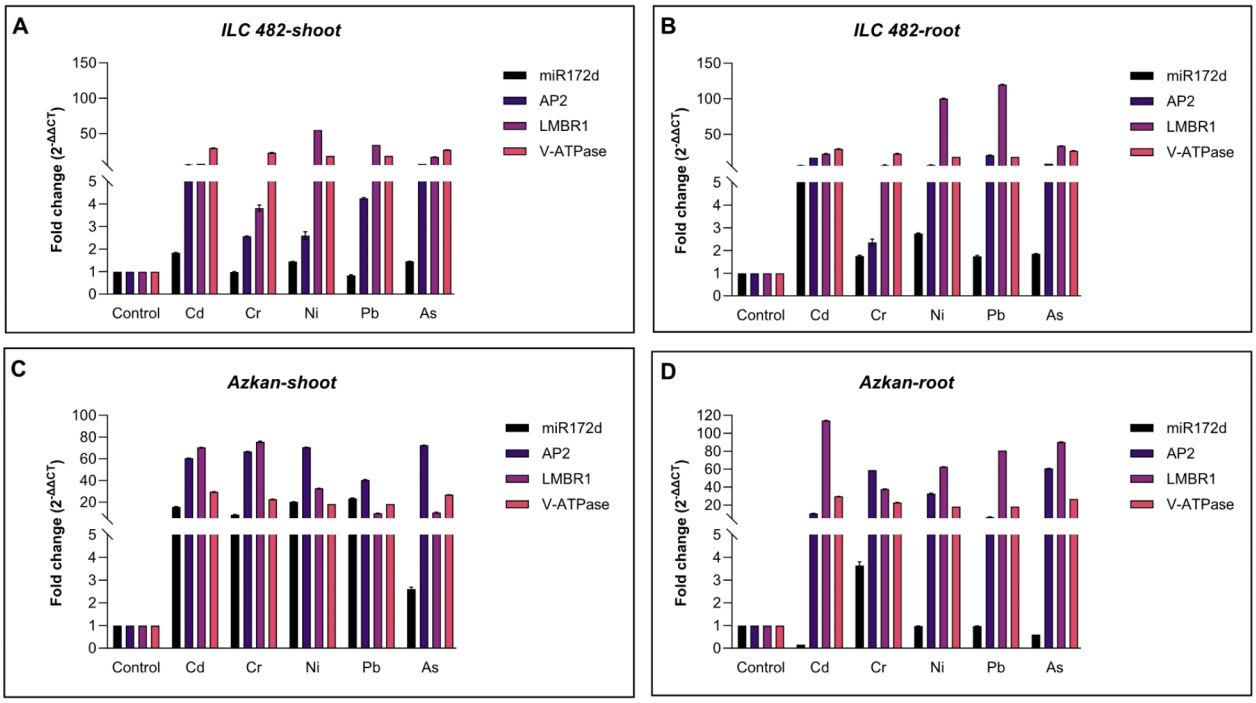

Fig. 10 Expression patterns of *car-miR172d* and its target genes under heavy metal stress. The bars are presented as mean ± SE ($n = 4$)

showed enhanced gene expression for *Ring Finger*, *AP2*, and *human UDP-glucose: glycoprotein glucosyltransferase (HUGT)* (Fig. 11).

In the ILC 482 genotype, the expression of *car-miR172f* was significantly elevated in shoot tissues under all treatments. In contrast, the increase in *miR172f* expression in root tissues was particularly prominent under Cd treatment. For the Azkan genotype, significant increases in *miR172f* expression were observed under Cd, Ni, and Pb treatments in shoot tissues, whereas root tissues exhibited notable increases specifically under Cr treatment. Furthermore, both the ILC 482 and Azkan genotypes in both tissue types showed increased expression of the *AP2* and *LMBR1* genes under metal stress conditions, with *LMBR1* showing the most substantial upregulation (Fig. 12).

The *car-miR172g* gene expression in shoot tissue of the ILC 482 genotype was markedly higher in treatments of Cr, Ni, and Pb than in control. Under Cr and Ni treatments, a significant increase was noted in root tissue. *car-miR172g* expression in shoot tissue of the Azkan genotype increased significantly only in response to As treatment. Under Pb and As treatments, higher expression levels were observed in root tissue. In addition, both genotype tissue types showed a significant increase in the expression level of *AP2* and *P4-ATPases*, the target genes of mir172g. Its expression in shoot tissue of the ILC 482 genotype showed variability depending on the treatments (Fig. 13).

Discussion

The impact of environmental stress on global agricultural production losses due to abiotic stress is becoming increasingly significant, resulting in a 70% decrease in output [60]. Heavy metal toxicity is a major abiotic stress that reduces plant biomass yield [61]. Non-essential hazardous metalloid chemicals such as As, Cd, Cr, Ni, and Pb have detrimental effects on crop productivity, quality, and human health [62–64]. Heavy metal toxicity has many effects on plants at the cellular and molecular levels. Heavy metal pollution harms plant root morphology, reducing plant development, chlorophyll content, levels of enzyme antioxidants, plant quality, and yield [65, 66].

Roots are the initial organs that encounter soils polluted with toxic metals [67]. The plants' expanded root systems could assimilate the metals due to the roots' water-absorbing capacity, which ultimately had a more significant negative impact on the roots [68]. The Azkan genotype had the highest shoot length loss in the As application group, while the ILC 482 genotype had a substantial shortening in the Cd application group. The shoot length of the Ni-treated groups was larger than that of the control group in both genotypes (Fig. S1A). In addition, the results revealed that heavy metals induced toxicity and significantly reduced the root length of the

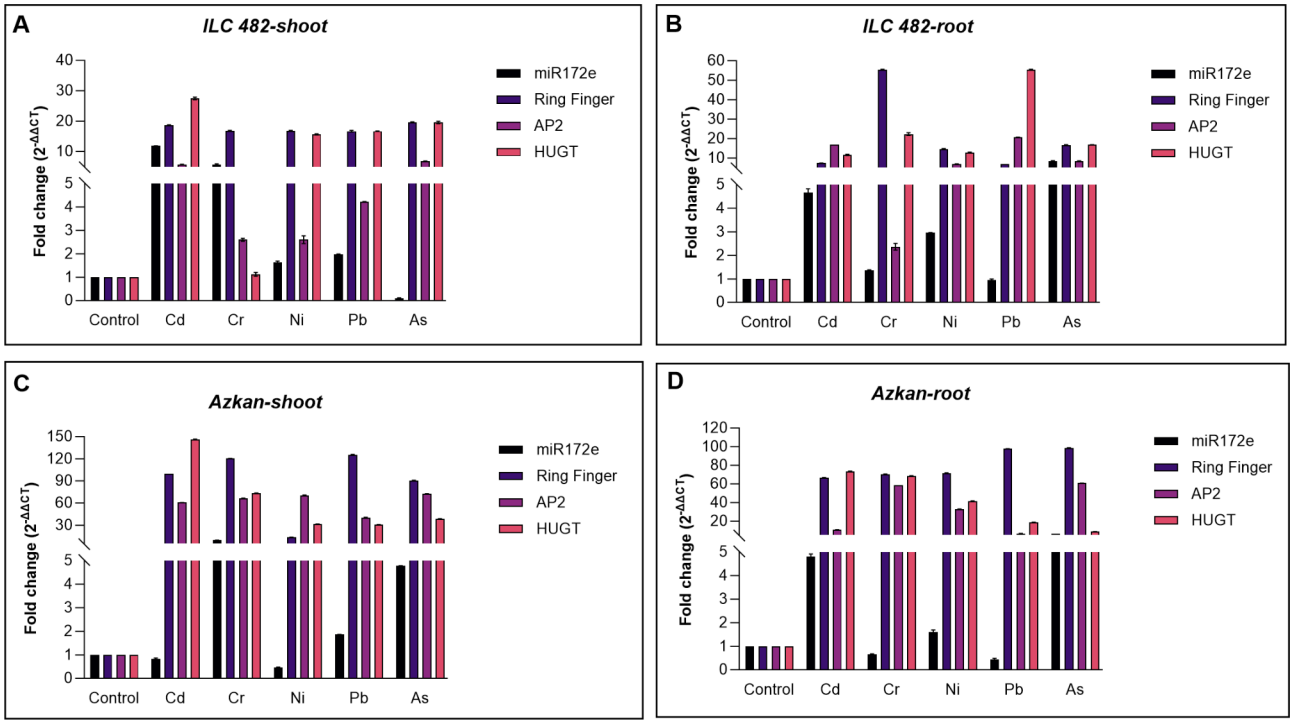

Fig. 11 Expression patterns of *car-miR172e* and its target genes under heavy metal stress. The bars are presented as mean ± SE ($n = 4$)

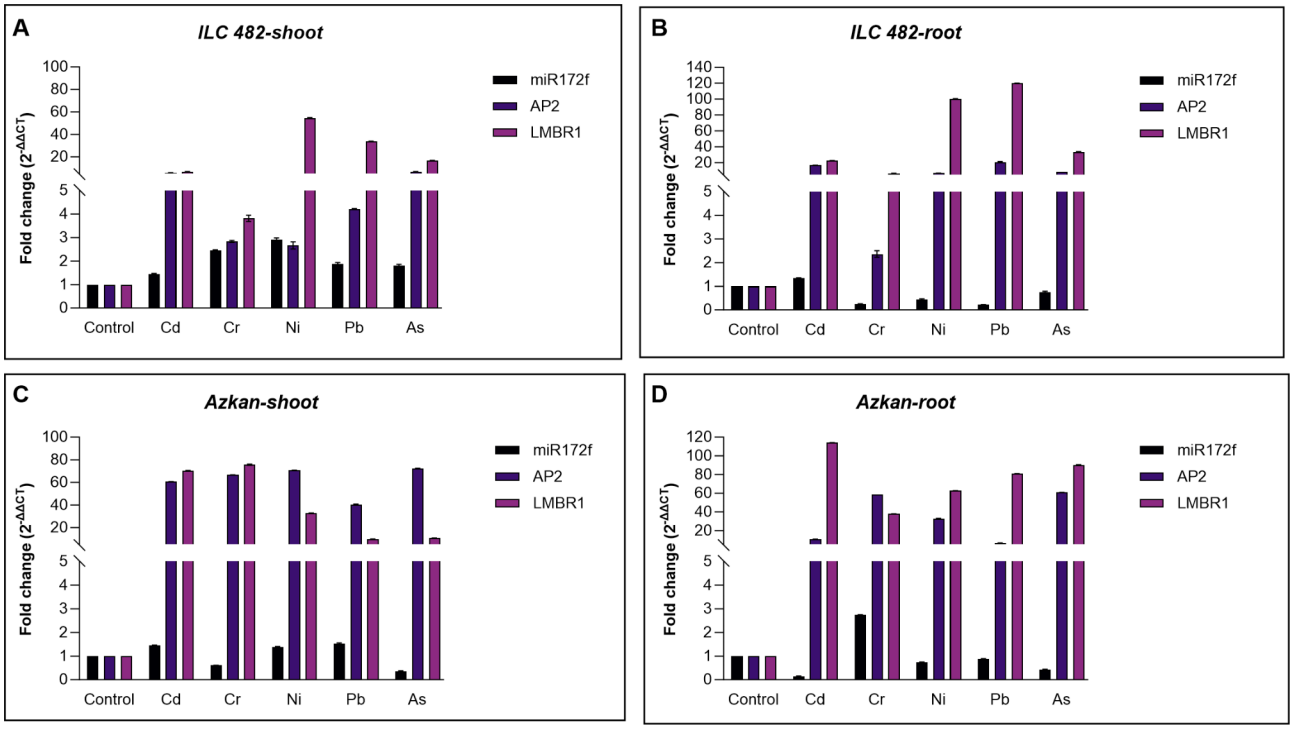

Fig. 12 Expression patterns of *car-miR172f* and its target genes under heavy metal stress. The bars are presented as mean ± SE ($n = 4$)

ILC 482 and Azkan cultivars. Both genotypes had the lowest mean root length after Cr and Cd treatments (Fig. S1B). The results that were obtained agree with the findings of other authors. Naz et al. [69] also reported a significant reduction in root and shoot length in chickpeas grown under increased doses of Cd, Cr, Zn, Ni, and Pb stress and all heavy metal combinations [68]. indicated that the toxicity of Cd, Cr, and Ni heavy metals in corn

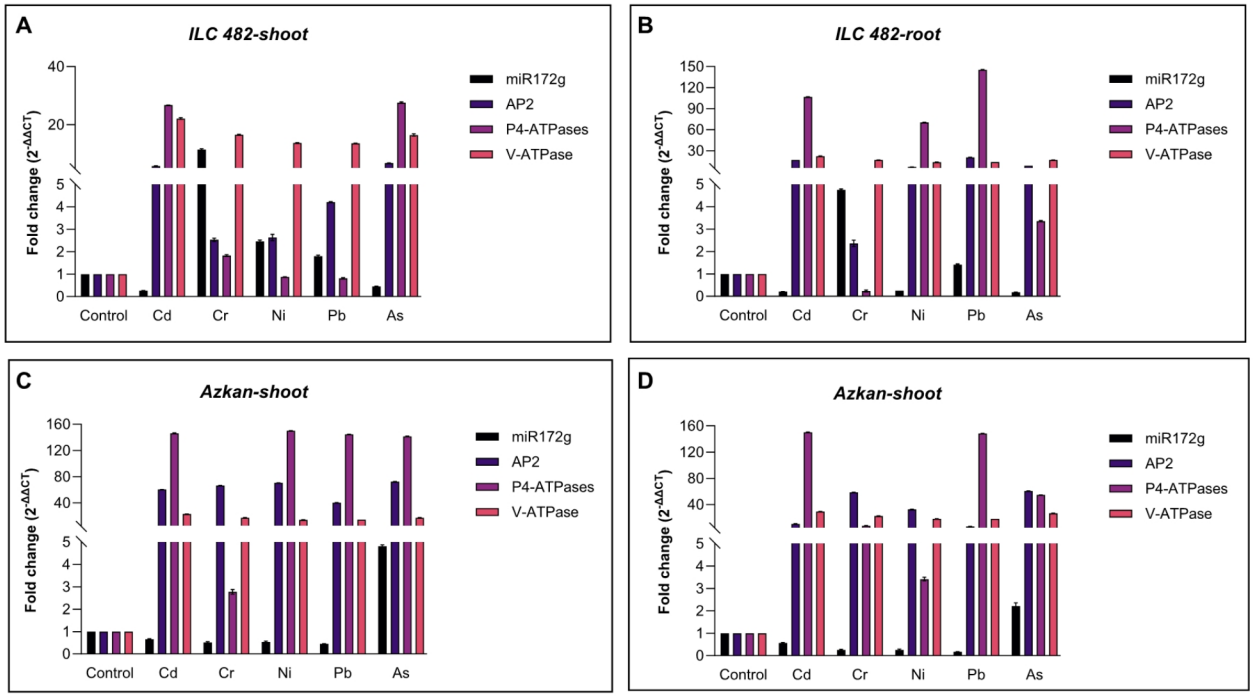

Fig. 13 Expression patterns of *car-miR172f*g and its target genes under heavy metal stress. The bars are presented as mean ± SE ($n = 4$)

increased with dose, and while all heavy metals reduced root length, Cd was the most effective on shoot growth, and Cr and Ni the least. As the As dose increased, shoot and root length gradually decreased [70]. In research on Cd toxicity in three chickpea types, Ullah et al. [71] found that 50 µM Cd stress reduced root and shoot length and fresh and dry weights.

One of the main effects of heavy metal toxicity on plants is damage to cell membranes, particularly the plasma membrane [72]. Heavy metals can damage membranes by oxidizing and cross-linking protein thiols, easily by binding the hydroxyl part of phospholipids, by replacing calcium ions at key locations on cell membranes, by stopping essential proteins like H^+-ATPase from working, or by changing the structure and flexibility of membrane lipids [73–76]. All those things lead to a drop in particular transporting activities and an increase in non-specific membrane permeability, which disturb ionic homeostasis and, in turn, the activities of several enzymes essential for fundamental cell metabolism [77]. All heavy metal applications increased CMD in both genotypes compared to the control group (Fig. S2).

Heavy metal toxicity can influence plasma membrane permeability, leading to a decrease in water content. In parallel with the results of CMD, it was determined that heavy metal applications caused a decline in RWC in both genotypes. Different research has declared that Cd, Cr, Ni, Pb, and As stress induces changes in plant water status in various plant species [78–82]. Furthermore, heavy metals can lead to severe dehydration in shots by limiting water movement from root parts to the shoot sections of plants [83]. In the Azkan genotype, the Cr application caused the highest decrease in RWC, while in the ILC 482 genotype, the Ni and Pb application caused the highest reduction in RWC (Fig. S3). Furthermore, RWC was a growth-related factor that affected PC1 (Fig. 2). This suggests that plants in control group (#3) grew and retained water better than those treated with heavy metals. The stability of water relations depends on the balance between transpiration and water uptake [84]. Ni toxicity decreased the area of plants' transpiring surfaces [85]. Excess Ni in plant tissues can cause chlorosis, necrosis, water potential and transpiration decreases, growth inhibition, and mortality [86]. Jagetiya et al. [87] indicated that leaves of green gram supplied with excess Ni (10, 100, and 1,000 µM) displayed a reduction in water potential (ψw) and RWC. Vezza et al. [88] reported that the treatment of soybean plants with As did decrease their leaf RWC and root WC compared to control plants. Zhang et al. [89] show that water deficiency reduces CC and photosynthetic rate in soybeans, decreasing plant height, biomass, and seed yield.

A high CC in plants is the basis for preserving the normal photosynthesis of mesophyll cells under stress [90]. The study observed a decrease in CC in all heavy metal applications in the sensitive genotype variety. In contrast,

a decrease was observed in only Cr and Pb applications in the tolerant variety. While Cd, Ni, and As reduced the CC content in the sensitive genotype, they increased the CC in the tolerant variety (Fig. S4). Piotto et al. [91] used the CC (SPAD index) as one of the metrics to assess the tolerance or sensitivity of tomatoes to Cd toxicity. Toxic Cd causes a drop in the number of chloroplasts or damage to the structure of the chloroplast, which speeds up the breakdown of chlorophyll and changes the plant's photosynthetic capacity [35]. Also, plants under Pb toxicity have their photosynthetic pathways negatively affected because it disrupts the ultrastructure of chloroplasts and blocks the synthesis of essential pigments, including chlorophyll and carotenoids, in addition to plastoquinone [73]. Cu and Pb at 800 µM inhibit chlorophyll and carotenoid biosynthesis and their incorporation into photosynthetic machinery [92]. Navabpour et al. [93] indicated that the leaf CC was reduced significantly in wheat cultivars under Pb stress. Reduced chlorophyll (a+b) levels may account for the decline in photosynthetic rates. Heavy metals capture electrons from the photosynthetic electron transport chain, generating harmful reactive oxygen species (ROS) [92].

Heavy metal toxicity leads to the excessive buildup of ROS within the cell [94]. In this context, heavy metals are divided into two: redox-active and redox-active [95]. Redox-active heavy metals, such as Fe, Cu, Cr, and Co, play a direct role in the redox processes that occur in cells. These metals are directly involved in the redox reaction that happens inside cells and leads to the production of $O_2^{\bullet-}$ and then H_2O_2 and OH through the Haber-Weiss and Fenton reactions [74]. Redox-inactive heavy metals such as Cd, Zn, Ni, and Al can indirectly produce ROS by inducing the expression of lipoxygenase (LOX) in plant tissues and causing the oxidation of indirect polyunsaturated fatty acids [75].

This study demonstrated that Cd, Cr, Ni, Pb, and As induce oxidative stresses by overproducing H_2O_2 (Fig. S5A and B) in the roots and leaves of chickpeas. This is in agreement with the results of the presence of Cd, Cr, Ni, Pb, and As, which induces oxidative stress in the developing parts of *Cicer arietinum* by increasing the production of ROSs [8, 96–99]. It is generally known that Pb stress binds thiol groups and alters cell redox state, increasing ROS generation [100]. Increased ROS accumulation through membrane lipid and protein disintegration leads to lipid peroxidation, one of the main causes of abiotic stress-induced cell damage [101, 102]. MDA is a lipid peroxidation product that indicates oxidative damage [103]. The increase in MDA content is directly related to increased H_2O_2 production, suggesting oxidative damage caused by excessive ROS production [104]. As a matter of fact, in our study, a positive correlation was determined between H_2O_2 and MDA amounts in both tissue types ($r=0.334$ at $p<0.05$ and $r=0.624$ at $p<0.01$ for shoot and root, respectively) (Fig. 1).

The process of priming or buildup of H_2O_2 in plant tissues enhances their tolerance to heavy metals by stimulating the antioxidant mechanism in their tissues [67]. Plants have a complex antioxidant system to maintain cellular redox balance; this protection's strength and potential depend primarily on the species and genotype [105]. An increase in SOD, CAT, and GR activities has been reported in Cd, Pb, Cu, and Zn-treated Pisum sativum root [106], SOD CAT, APX, GR, POD, GST, GPX, DHAR, and MDHAR in V, Cr, Ni, and Cd-treated pepper leaves [107], SOD, CAT, POD, and APX in Cd, Pb, and Ni-treated common bean [108].

All antioxidative enzymes showed parallel activity patterns in shoots and roots globally. The study found that the SOD enzyme activity was typically higher in root and shoot organs of two different genotypes (Fig. S6A and B). This outcome was expected, as other studies have already shown similar findings [101, 109–112]. Results indicated a positive correlation between the increase in SOD activity and H_2O_2 levels (Fig. 1). This may be explained by the fact that an increase in $O_2^{\bullet-}$ levels increases SOD activity, leading to the acceleration of $O_2^{\bullet-}$ degradation and consequently elevating the H_2O_2 content [113]. The application of Ni led to the highest increase in the root tissue of the sensitive genotype (Fig. S6A and B). Ni is involved in the composition of enzymes such as superoxide dismutases, glyoxalase, peptide deformylase, methyl-CoM reductases, urease, and some hydrogenases [73].

Exposure to Cd, Cr, Ni, Pb, and As increased CAT activity in both tissues of ILC 482 and Azkan genotype compared to control plants (Fig. S6C and D). A positive correlation was determined between CAT and H_20_2, especially root tissue exposed to heavy metal (Fig. 1). CAT is a crucial enzyme that defends biomolecules from oxidative damage by decomposing H_2O_2 into water and oxygen [114]. Furthermore, the treatments with Cd and Cr showed a strong correlation with PC1 according to the results of the PC analysis (Fig. 2). These treatments were explicitly associated with CAT and Proline, which are oxidative stress responses. CAT is closely related to PODs, both structurally and functionally. It has two functions: it reacts "peroxidatically" at lower concentrations of peroxide and "catalytically" at higher concentrations [115]. Figure 1 has been examined, revealing a positive correlation between CAT and POD. Other studies supported the increase in CAT activities with Cd, Cr, Ni Pb, and As applications compared to the control [116–119].

POD is found in many plant tissues and organs, removes peroxides, inhibits membrane lipid peroxidation, and prevents membrane damage [120]. The levels of POD were increased after all heavy metal treatment (Fig. S6C and D). Upon metal ions' entry into the plant body,

a rapid accumulation of toxic compounds ensues, leading to an increase in the substrate of the POD enzyme [121]. Kang et al. [122] observed increased POD levels in potatoes under Cd stress, which supports our results. Treatments with concentrations of As 5, 25, and 125 µM in broccoli considerably enhanced the activity of CAT and POD enzymes [123].

APXs catalyze the reduction of H_2O_2 to water and serve a crucial function in plants' antioxidant systems [124]. In our findings, all treated increased the activity of APX in chickpeas. Shortly, the highest APX enzyme activity was seen in the shoots/roots of chickpeas treated with As in the sensitive genotype (ILC 482) compared to the control (Fig. S6E and F). Ibrahim et al. [125] indicated higher APX levels in wheat seedlings under As stress, which supports our findings. Moreover, there was a positive and significant correlation ($r=0.599$ and $r=0.594$ at $p<0.01$ for shoot and root tissues, respectively) between H_2O_2 and APX levels in both tissues (Fig. 1). In response to abiotic stress, plants release the intracellular signal H_2O_2, which effectively activates APX, contributing to the plant's ability to cope with and adapt to stress [126].

Plants not only produce antioxidants to protect themselves, but they also create a variety of cellular biomolecules that serve as compatible and metabolic osmolytes. These biomolecules, like proline, help maintain osmotic equilibrium and counteract the harmful effects of metal toxicity [4]. Excessive cell proline accumulation is a sign of stress, and plants exposed to biotic and abiotic challenges frequently accumulate proline as a protective mechanism [127]. Proline is an osmoregulatory component and acts as a chaperone molecule to stabilize proteins and scavenge ROS [128, 129]. Plants' ability to accumulate proline under heavy metal stress might be influenced by the direct effects of metal ions and water shortage [130]. This study showed proline accumulation in chickpea shoots and roots under the influence of heavy metals, and this accumulation was found to depend on the applied heavy metal dose and organs. Bushra et al. [131] show that the proline concentration of chickpea plants significantly increased in the highest Cd (100 mg kg^{-1} soil) level as compared with untreated plants, as that of [132] in chickpeas under Cd and Pb, of [133] in finger millet under As and Ni. The tolerant Azkan genotype showed higher proline accumulation in other heavy metals, except for Ni and Pb heavy metals. Plants that are tolerant to stress have a higher concentration of proline than those that are sensitive to stress [134]. Under Cr (120 µM) stress, two varieties of chickpeas showed increases in proline accumulation in their roots and leaves compared to control plants, with the tolerant genotype showing these more pronouncedly than the sensitive genotype (Fig. S7A and B).

Plants have evolved complex molecular defense mechanisms that include physiological mechanisms and gene regulation to cope with abiotic stress [135]. This defense mechanism can be effectively achieved through the interaction of multiple genes, cofactors, and miRNAs [136]. The mRNA profiles of the antioxidant enzymes encoding POD, CAT, and APX were studied to evaluate the antioxidative responses to heavy metal stresses applied in the study. Compared to control plants, both genotypes' mRNA expression levels of antioxidant enzyme genes rose in response to Cd, Cr, Ni, Pb, and As stress (for the *CAT* gene, except for the Azkan genotype's Cd application in root tissue) (Fig. S8). However, the expression of antioxidant enzymes such as SOD, CAT, and APX in heavy metals stressed environments has been shown to play an essential role in reducing heavy metal toxicity, as reported in studies under various plant species. In this connection, Sharma et al. [137] and Alwutayd et al. [138] reported the increased activities of SOD, CAT, and APX at Cr treatment in rice [93]. observed increased antioxidant enzyme activity (SOD, CAT, GPX, and APX) and gene overexpression in wheat leaf and root tissues under Pb stress. After 14 days of Ni stress in *Leersia hexandra* the expression of *APX7*, *SODCP*, *SOD1*, and *CAT* genes were significantly upregulated. Still, the expression of the glutathione metabolic cycle was reported to be downregulated [139]. The treatments of 160, 320, and 1280 µM of Cd^{+2} in tomato increased the expression level of the *Cat2* gene compared to the control [140]. Transcript levels of LOX and SOD were significantly ($p<0.05$) upregulated during 25 µM As exposure in rice [141].

Understanding these mechanisms is crucial for developing strategies to improve plants' stress tolerance. Despite gene function being regulated at various steps, miRNAs' post-transcriptional transcript level regulation adds complexity to the mechanism [142]. miR172 was first comprehensively revealed in chickpeas under abiotic stress, shedding light on previously undiscovered genetic factors in this important plant species. The miR172 family is found in several plants; however, the number of members differs within plant kingdoms. In this study, 7 *miR172* genes were identified in chickpeas (Table 3). Previous studies have identified 5 *miR172* gene family members in *A. thaliana* [56, 143, 144], 4 in *O. sativa* [145, 146], 3 in *H. vulgare* [147], and 12 in *G. max* [148]. The *car-miR172* gene family members are on five chickpea chromosomes (Fig. 3). Bansal et al. [57] demonstrated that the *miR172* genes are unevenly distributed among only five (chromosomes 4, 5, 6, 9, and 11) out of the twelve chromosomes in tomato. In *A. thaliana*, *miR172* genes have been identified on chromosomes 2, 3, and 5 [56]. Secondary structural determinants of the precursors, such as the sequences surrounding the miRNA region and stem-loops bulges, are crucial for

miRNA processing [149–151]. This study revealed that every gene possesses the essential hairpin structure for the formation of miRNA (Fig. 4). *miR172* gene family members in *Elaeis guineensis* also have a hairpin structure, and similarly, mature sequences are located close to the ends [152]. The four precursor sequences' *bna-mirl72* gene transcript secondary structures created varied stem-loop structures, which may affect member function [153]. The alignment of mature miR172 sequences demonstrates that seven mature miR172 sequences are highly conserved, with variations occurring only in the first, last, and medium bases (Fig. 5). Differences or similarities in mature sequences may lead to variations in functional abilities [154]. The results of the motif composition of car-miR172 strongly supported its classification through phylogenetic analysis. Analyzing the amino acid sequences of the conserved miR172 domain from *C. arietinum*, *A. thaliana*, *G. max*, *O. Sativa*, and *M. truncatula* revealed distinct classifications into three different groups, providing insights into their evolutionary relationships (Fig. 6). The *car-miR172* genes belong to the same group and are closely related to other species and each other. Similar results were found in a study where a phylogenetic tree was constructed for all leader sequences of miR172 in the AA, BB, and CC genomes of *Brassica* and divided into three classes [155]. The phylogenetic analysis of the pioneer regions of miR172 between *Oryza sativa* and six wild cousins showed that three evolutionary branches emerged [156].

Numerous conserved and species-specific miRNAs linked to stress responses have been discovered in various crops [157–159]. When plant organs are exposed to heavy metal stress, many dysregulated miRNAs and the genes they target play crucial roles [160]. In plants, miRNAs responsive to metal stress are identified in multiple sets along with their targets [161]. Nevertheless, the miRNA and their target gene expression profiles in chickpea organs still need investigation in response to heavy metal stresses. During heavy metal stress, miRNAs selectively target different genes engaged in metabolic pathways related to metal stress response. These processes include the signaling of phytohormones, the absorption and distribution of sulfates, the activation of antioxidant scavengers, and the synthesis of miRNAs [162, 163]. In accordance with previous studies, the majority of the predicted target genes of various conserved and novel miRNAs were found to encode TFs such as NAC, AP2, NFYA5, ARF, MADS, bHLH, MYB, WRKY, NAC, DREB, and SPL [154, 164–166].

The results grouped the expression of miR172 members and their target genes (*FtsH*, *Ring Finger*, *AP2*, *P4-ATPase*, *HUGT*, *ATX1*, *V-ATPase*, and *LMBR1*) into up-regulated, down-regulated, and genes with no significant change in gene expression (Figs. 7, 8, 9, 10, 11, 12 and 13). Seven members of the car-miR172 family, namely car-miR172a, b, c, d, e, f, and g, potentially target *AP2* genes (Tables S2). Moreover, these genes also showed different expression levels in the root and shoot tissues of the two genotypes (sensitive and tolerant) when under heavy metal stress. miRNAs were expressed differently between 2 genotypes against Cr stress in tobacco, which indicates the diversity in their genetic structures and different responses [167]. Additionally, the expression of target genes was determined to be higher than car-miR172a (Fig. 7). It is known that upregulation of miRNAs leads to downregulation of their target mRNAs, and the opposite can occur in a stressful environment [168]. Yu et al. [169] identified different As-responsive miRNAs in rice, revealing that these genes are involved in transport, signaling, and metabolic processes.

Lower expression of miR172a, miR172c, and miR172d in Azkan than in ILC 482 may partly explain the high As tolerance of Azkan. Under As (III) stress, decreased expression of miR172 with concomitant increased expression of AP2-like transcripts has been reported [170]. In *Aquilaria sinensis*, the expression level of *AsERF1* increased under Cd stress, reaching 3.5-fold at the highest point compared to the control group [171]. Interestingly, miR172b and *FtsH*, *AP2*, and *ATX1* target genes were increased in both tissues of both genotypes in all treatments (Fig. 8). Inal et al. [172] investigated the expression of the *PvFtsH* gene in response to drought and salt stress in beans. They revealed that it can respond to environmental and physiological stress factors. The expression of miR172 in cotton was decreased by 50 µM Pb but increased by 100 and 200 µM Pb treatments. It has also been reported that specific miRNAs and target genes (*miR414–RAX1*, *miR833a–RAX2* and *miR5658–BIT1*) showed a positive correlation in root tissue except at 100 µM Pb concentration [173]. Both *miR319* and *miR159* showed upregulation under Ni stress conditions in castor beans.

In all experimental conditions involving heavy metal treatments, the expression of *V-ATPase*, a gene targeted by car-miR172c and car-miR172d, exhibited increased activity across all genotypes and tissue types (Figs. 9 and 10). *V-ATPases* enhance gene expression and transport activity in cucumber and barley when exposed to heavy metals [174]. The expression levels of *Ring Finger*, *AP2*, and *HUGT* target genes, which car-miR172e regulates, were elevated, regardless of car-miR172e expression in all treatments (Fig. 11). In transgenic lines overexpressing the *Ring Finger* gene in *S. lycopersicum* exposed to Cd stress, Cd accumulation in shoots and roots decreased, and antioxidant activity genes like *CAT*, *DHAR*, and *MDHAR* were increased, increasing the plant's tolerance to heavy metal stress [175]. In the ILC 482 genotype, car-miR172f showed an increased expression profile in shoot

tissue under all stresses, while it showed a decreased expression profile in root tissue under all stresses except Cd stress. In addition, the *LMBR1* gene exhibited the highest expression profile in Cd application in root tissue (Fig. 12). *miR172f*, *miR398*, and *miR857* were reported to be up-regulated under 80 µM $CdCl_2$ stress in *Brassica napus* [176]. car-miR172g expression was down-regulated in both genotypes and tissues (Fig. 13). miR172, which targets TFs such as AP2, has also been reported to be down-regulated by Cd in *Solanum torvum* roots [177]. This strong evidence suggests that miRNA regulates the response to environmental factors, contributing to the plant's overall resilience. With its unique perspective, this research will be a starting point for understanding the regulatory mechanisms and biological functions of the identified miRNAs and their target genes in the future.

Conclusion

This study describes in great detail how heavy metal stress affects two types of chickpeas, ILC 482 and Azkan. It shows that growth, physiological, and biochemical parameters significantly differ depending on the genotype and treatment. When root length was evaluated, Cr and Cd applications exhibited the lowest root length averages compared to other metal applications in both genotypes. Metal stressors caused cell membrane damage and decreased relative water and chlorophyll content, indicating significant physiological disturbances. Biochemically, H_2O_2 and MDA levels were elevated, along with antioxidant enzymes like SOD, CAT, POD, and APX and non-enzymatic molecules like proline, indicating a robust antioxidative response to oxidative stress. The study found seven *miR172* genes in the chickpea genome: car-miRNA172a, b, c, d, e, f, and g. The genes are spread across five chromosomes and share hairpin structures necessary for miRNA processing. These miR172s are involved in heavy metal stress and identified their possible target genes, such as *AP2*, *FtsH*, *ATX1*, *P4-ATPase*, *V-ATPase Ring Finger*, *HUGT*, and *LMBR1*, which may serve as TFs in various stress response pathways.

miR172 plays a significant role in the molecular response to heavy metal stress in plants, but further functional validation using gene knockdown or overexpression experiments is necessary to illuminate its precise regulatory mechanisms. Advanced techniques like CRISPR/Cas9 for genome editing can provide deeper insights into miR172's role and uncover additional pathways involved in stress tolerance, ultimately helping produce heavy metal-resistant chickpeas. The results can be used in breeding programs to develop stress-tolerant chickpea varieties, especially for agricultural areas contaminated with heavy metals. miRNA-based genetic engineering methods are an essential tool in such breeding studies. Moreover, extending research through field experiments and cross-species analysis can help translate laboratory findings into practical agronomic solutions. Exploring the interactions between miR172-regulated pathways and phytohormones like ABA, ethylene, and auxin is essential for a deeper understanding of stress modulation in chickpeas. To better understand the response of miR172 and its pathways to multiple stress factors, it is important to understand its role in other abiotic stresses besides heavy metal stress.

Methods

Plant material and design of experiment

This study used seeds of Azkan (tolerant) and ILC 482 (sensitive) genotypes as plant materials. Azkan and ILC 482 genotypes were obtained from the Transitional Zone Agricultural Research Institute in Eskisehir, Turkey, and the GAP International Agricultural Research and Training Center in Diyarbakir, Turkey, respectively.

The seeds of these two genotypes were sterilized with sodium hypochlorite (10%) for 5 min and washed three times with pure water. Sterilized seeds were grown in 70×50×15 cm sized perlite-containing germination boxes for 12 days under controlled conditions in a plant growth chamber with 250 mmol at 25 °C and a 16-hour photoperiod. The plant seedlings were raised for three weeks in a hydroponic system (pH=5.5–5.7) using a half-strength Hoagland solution [71, 178]. Then, treatments [control (no heavy metals), 100 µM $Cd(SO_4)_2$, 100 µM $K_2Cr_2O_7$, 100 µM $NiSO_4.6H_2O$, 100 µM $Pb(NO_3)_2$, and 30 µM $NaAsO_2$] were applied with half-strength Hoagland solution. One preliminary experiment was performed to determine the heavy metal concentrations of chickpeas. For this, the standard LC_{50} method was employed, which represents the concentration at which half of the maximal growth of the chickpea root is inhibited. The research was established according to a randomized trial plan with three replications and ten plants in each replication. Plants were harvested seven days [128] after treatment and shoot length (SL) and root length (RL) were measured. Plant samples (shoots and roots) were frozen with liquid nitrogen and stored at -80 ∘C until biochemical and molecular analysis.

Cell membrane damage (CMD %)

CMD was performed according to Lutts et al. [179]. The calculation of cell membrane damage in the treatment groups was determined using the following formula.

$$\mathrm{CMD}(\%) = (\mathrm{EC1}/\mathrm{EC2}) \times 100.$$

Relative water content (RWC %)

To determine the RWC ratio in leaf tissue, four leaf samples were selected from each replicate group of

treatments, and their fresh weights (FW) were measured. Then, the leaf samples were soaked in pure water for 4 h, and their turgor weights (TW) were determined. They were kept in an oven at 80 °C for 48 h, and their dry weights (DW) were measured. The RWC (%) was determined using the following formula [180].

RWC (%): [(FW – DW) / (TW – DW)] x 100.

Chlorophyll content (CC) (SPAD)

SPAD-502 (Chlorophyll Meter; Konica Minolta, Tokyo, Japan) was used to determine CC. This device measured leaf transmittance at 650/940 nm electromagnetic spectrum wavelengths. Readings were taken by chance in the middle parts of 5 plants' upper leaves using the SPAD-502 device [181, 182].

Hydrogen peroxide (H2O2), malondialdehyde (MDA), and antioxidant activities

H_2O_2 and MDA levels were determined in shoot and root tissues using the methodology described by Shams et al. [183]. The H_2O_2 concentration was measured by employing a standard calibration curve, which involved utilizing various concentrations of H_2O_2. The MDA concentration was determined by measuring the levels of thiobarbituric acid-reactive chemicals and calculating it from the absorbance curve using an extinction coefficient of 155 mmol L^{-1} cm^{-1}. The antioxidant enzyme activities (SOD, CAT, POD, and APX) were measured on fresh leaf samples using the techniques of Shams et al. [183].

Proline content

Proline content was determined according to the method used by [184, 185]. Fresh shoot and root tissues (0.1 g) were homogenized with sulphosalicylic acid (3%) (2 mL) and heated at 100 °C by adding glacial acetic acid (1 mL) and Ninhydrin reagent (1 mL). Then, toluene was added to the cooled samples, and readings were taken at 520 nm wavelength. The proline level in shoot and root tissues was evaluated with a standard curve constructed from pure proline.

Statistical analysis of morphological, physiological, and biochemical characters

Data was subjected to a two-way analysis of variance using the Minitab 19.2.0 program according to a completely randomized experimental arrangement in 2 (Genotype; G) x 6 (Treatment; T) factorial design. Tukey's HSD (honestly significant difference) test was used to identify differences between means at 0.05 level. A simple main effect explained the GxT interaction effect. Correlation analysis used the Pearson correlation test (two-tailed) to reveal the relationships among examined variables. Graphical analysis was performed using Origin 2021b software (OriginLab Cooperation, Northampton, MA, USA). Using a correlation matrix, a principal component analysis (PCA) was used to detect loading values using GraphPad Prism software, version 9.5.1. The PCA results were visually represented by constructing biplots generated using GraphPad Prism software, version 9.5.1.

Identification and classification of *miR172* genes family in chickpea

miR172 precursor and mature sequences in all plants (*C. arietinum*, *A. thaliana*, *G. max*, *O. sativa*, *and M. truncatula*) were searched for using sRNAanno (http://www.plantsrnas.org) and PmiREN 2.0 database (Table S1) [186, 187]. The positions of *miR172* gene family members on chickpea chromosomes were scanned on the genome of *C. arietinum* (https://phytozome-next.jgi.doe.gov/info/Carietinum_v1_0) using the BLAST tool in the Phytozome v13 database [188]. The obtained chromosome information was visualized using the MG2C v2.1 (http://mg2c.iask.in/mg2c_v2.1/) web tool [189]. The RNAfold Web Server (http://rna.tbi.univie.ac.at/cgi-bin/RNAWebSuite/RNAfold.cgi) web tool was used to predict the secondary structures of *car-miR172* gene family members [190].

Identification of conserved motifs and phylogenetic analysis of the car-miR172 family members

Using the mature sequence information of car-miR172 family members, conserved regions were visualized with the SeqLogo tool in TBtools [191]. To construct a phylogenetic tree among *C. arietinum*, *A. thaliana*, *G. max*, *O. Sativa*, and *M. truncatula* plants, the leader sequences of *miR172* genes obtained from the sRNAanno database were aligned using the ClustalW tool [192]. Then, the MEGA 11 program was used [193]. The created phylogenetic tree was visualized with the help of the Evolview v2 web tool [194].

Prediction of genes that may be targets of car-miR172

The target genes of car-miR172 were predicted with the help of the psRNATarget [195] database using default settings (Table S2). The settings in the psRNATarget database were: Maximum expectation 4.0 (Range: 0–5), length for complementarity scoring 20 (Range: 15–30 bp), Target accessibility 25.0 (Range: 0-100), Flanking length around target site for target accessibility analysis 17, Range of central mismatch leading to translational inhibition 9–11 nt. The matching gene car-miR172 gene family members were targeted, and the miRNA-target gene relationship was determined.

Expression analysis of the *car-miR172* family, target, *APX*, *CAT*, and *SOD* genes in chickpea

Total RNA isolation in shoot and root tissues was performed with Trizol® Reagent. According to the

manufacturer's procedure, the SuScript cDNA Synthesis Kit (CAT: RT01A025) was used to synthesize cDNA (complementary DNA). Furthermore, unlike cDNA synthesis of other genes, miRNA-cDNA synthesis was performed using miRNA-specific stem-loop RT primer (Tables S1) [143]. qRT-PCR analysis was conducted with the RotorGene® Q Real-Time PCR System. 2X SuYBR-Green qPCR Mastermix (CAT: PCR01C0252, Ankara, Turkey) mix was 20 µl in total, including cDNA (100 ng) 4 µL, primer (forward+reverse) 1 µl, SYBR green master mix 10 µL, and dH_2O 5 µl. The reaction was carried out as follows: 95 °C for 5 min, followed by 40 cycles of 95 °C for 10 s, 55 °C for 15 s, and 72 °C for 20 s. Genes were amplified from four biological replicates, with three technical replicates for each one.

Sequence information of the primers used in the study is shown in Tables S1 and S2. Primers were designed using the web-based Primer3 (http://bioinfo.ut.ee/primer3-0.4.0/) program. The specificity of the primers was tested using PCR, which was visible on a 1.2% agarose gel, as well as their product qRT-PCR melting curves. To evaluate the normalization of expression, the actin gene was used for *APX*, *CAT*, and *SOD* genes, while the *U6* gene [196] was used for target genes. At the same time, expression measurements of the *miR172* gene family were normalized according to the weighted average normalization method [197]. The $2^{-\Delta\Delta CT}$ normalization formula developed by [198] was used to analyze fold changes in gene expression. The data's averages and standard deviation values were obtained in the study using four replicates, and Data were visualized with GraphPad Prizm 8. Means were compared to the control group using Dunnett's test.

Abbreviations

APX	Ascorbate peroxidase
AP2	Apetela2
ATX1	Arabidopsis Homolog of Trithorax
CAT	Catalase
FtsH	Filamentation temperature-sensitive H
HUGT	Human UDP-glucose: glycoprotein glucosyltransferase
H_2O_2	Hydrogen peroxide
LMBR1	Limb development membrane protein-1
MDA	Malondialdehyde
microRNA	miRNA
PCA	Principal component analysis
P4-ATPase	P-type ATPases
SOD	Superoxide dismutase
V-ATPase	V-type ATPases

Supplementary Information

The online version contains supplementary material available at https://doi.org/10.1186/s12870-024-05786-y.

Supplementary Material 1

Supplementary Material 2

Acknowledgements
The authors are thankful for the financial support provided by Atatürk University.

Author contributions
Research concept and design: MA, EI, AC, and EY; Performed experiments: SU, EY, and BMO; Data analysis: MA, SU, EY, and AGK; visualization: SU, BMO, AC, and MA; Preparation of the draft manuscript: SU, EY, MA; Review and editing: EY, EI, EY and MA. All authors have reviewed and approved the published version of the manuscript.

Funding
This research was supported by the Atatürk University Scientific Research Project Coordination Unit under project number FYL-2023-12102.

Data availability
The authors state that data supporting this investigation's findings are included in the article. If raw data files are requested, they are available from the respective author upon reasonable request.

Declarations

Ethics approval and consent to participate
Not applicable.

Clinical trial number
Not applicable.

Consent for publication
Not applicable.

Competing interests
The authors declare no competing interests.

Author details
[1]Department of Molecular Biology and Genetics, Faculty of Science, Erzurum Technical University, Erzurum, Turkey
[2]Department of Agricultural Biotechnology, Faculty of Agriculture, Ataturk University, Erzurum, Turkey
[3]Department of Horticulture, Faculty of Agriculture, Ataturk University, Erzurum, Turkey

Received: 4 September 2024 / Accepted: 5 November 2024
Published online: 12 November 2024

References

1. Vignesh K, Yadav DK, Wadikar D, Semwal A. Exploring sustenance: cereal legume combinations for vegan meat development. Sustain Food Technol. 2024;2(1):32–47.
2. Oparah IA, Hartley JC, Deaker R, Gemell G, Hartley E, Kaiser BN. Symbiotic effectiveness, abiotic stress tolerance and phosphate solubilizing ability of new chickpea root-nodule bacteria from soils in Kununurra Western Australia and Narrabri New South Wales Australia. Plant Soil. 2024;495(1):371–89.
3. Usman M, Xu M. Plant-Based Proteins: Plant Source, Extraction, Food Applications, and Challenges. In: Du X, Yang J, editors. Flavor-Associated Applications in Health and Wellness Food Products . Springer, Cham; 2024. 253-94
4. Cheema A, Garg N. Arbuscular mycorrhizae reduced arsenic induced oxidative stress by coordinating nutrient uptake and proline-glutathione levels in Cicer arietinum L.(chickpea). Ecotoxicol. 2024;33(2):205–25.
5. Ahmad M, Naseer I, Hussain A, Zahid Mumtaz M, Mustafa A, Hilger H, Ahmad Zahir T, Xu Z. Appraising endophyte–plant symbiosis for improved growth, nodulation, nitrogen fixation and abiotic stress tolerance: an experimental investigation with chickpea (Cicer arietinum L). Agron. 2019;9(10):621.
6. FAOSTAT Statistical Database. http://www.fao.org/faostat/en/#data. Accessed 16 Oct 2024.
7. Islam MR, Biswas L, Nasim S, Islam MA, Haque MA, Huda AN. Physiological responses of chickpea (Cicer arietinum) against chromium toxicity. Rhizosphere. 2022;24:100600.

8. Singh D, Sharma NL, Singh CK, Sarkar SK, Singh I, Dotaniya ML. Effect of chromium (VI) toxicity on morpho-physiological characteristics, yield, and yield components of two chickpea (Cicer arietinum L.) varieties. PLoS ONE. 2020;15(12):e0243032.
9. Gaur VK, Sharma P, Gaur P, Varjani S, Ngo HH, Guo W, Chaturvedi P, Singhania RR. Sustainable mitigation of heavy metals from effluents: toxicity and fate with recent technological advancements. Bioengineered. 2021;12(1):7297–313.
10. Niekerk LA, Gokul A, Basson G, Badiwe M, Nkomo M, Klein A, Keyster M. Heavy metal stress and mitogen activated kinase transcription factors in plants: exploring heavy metal-ROS influences on plant signalling pathways. Plant Cell Environ. 2024.
11. Grobelak A, Kowalska A. Heavy metal mobility in soil under futuristic climatic conditions. In: Parasad MNV, Pietrzykowski M, editors. Climate Change and Soil Interactions. Elsevier; 2020: 437-451.
12. Alengebawy A, Abdelkhalek ST, Qureshi SR, Wang M-Q. Heavy metals and pesticides toxicity in agricultural soil and plants: ecological risks and human health implications. Toxics. 2021;9(3):42.
13. Kanwar VS, Sharma A, Srivastav AL, Rani L. Phytoremediation of toxic metals present in soil and water environment: a critical review. Environ Sci Pollut Res. 2020;27:44835–60.
14. Ungureanu EL, Mustatea G. Toxicity of heavy metals. In: Environmental impact and remediation of heavy metals. IntechOpen; 2022.
15. Kumar P, Naik M, Kumar T. Cadmium induced alteration in leaf number, stem girth and branch number of chickpea. Plant Arch. 2020;20(2):3430–5.
16. El-Sappah AH, Rather SA. Genomics approaches to study abiotic stress tolerance in plants. In: Aftab T, Hakeem KR, editors. Plant Abiotic Stress Physiology: Volume 2: Molecular Advancements (1st ed.). Apple Academic Press; 2022. p. 25–46.
17. El-Sappah AH, Zhu Y, Huang Q, Chen B, Soaud SA, Abd Elhamid MA, Yan K, Li J, El-Tarabily KA. Plants' molecular behavior to heavy metals: from criticality to toxicity. Front Plant Sci. 2024;15:1423625.
18. Khalef RN, Hassan AI, Saleh HM. Heavy metal's environmental impact. In: Environmental impact and remediation of heavy metals. IntechOpen; 2022.
19. Ahmed SF, Kumar PS, Rozbu MR, Chowdhury AT, Nuzhat S, Rafa N, Mahlia T, Ong HC, Mofijur M. Heavy metal toxicity, sources, and remediation techniques for contaminated water and soil. Environ Technol Inno. 2022;25:102114.
20. Kapoor RT, Mfarrej MFB, Alam P, Rinklebe J, Ahmad P. Accumulation of chromium in plants and its repercussion in animals and humans. Environ Pollut. 2022;301:119044.
21. Kumar T, Tedia K, Samadhiya V, Kumar R. Review on effect of fly ash on heavy metals status of soil and plants. Int J Chem Stud. 2017;5(4):11–8.
22. Necibi M, Mzoughi N. The distribution of organic and inorganic pollutants in marine environment. Micropollutants: sources, ecotoxicological effects and control strategies; 2017. p. 129.
23. Shreya D, Jinal HN, Kartik VP, Amaresan N. Amelioration effect of chromium-tolerant bacteria on growth, physiological properties and chromium mobilization in chickpea (Cicer arietinum) under chromium stress. Arch Microbiol. 2020;202:887–94.
24. Cuypers A, Hendrix S, Amaral dos Reis R, De Smet S, Deckers J, Gielen H, Jozefczak M, Loix C, Vercampt H, Vangronsveld J. Hydrogen peroxide, signaling in disguise during metal phytotoxicity. Front Plant Sci. 2016;7:470.
25. Zhao F-J, Tang Z, Song J-J, Huang X-Y, Wang P. Toxic metals and metalloids: Uptake, transport, detoxification, phytoremediation, and crop improvement for safer food. Mol Plant. 2022;15(1):27–44.
26. Ningombam L, Hazarika B, Yumkhaibam T, Heisnam P, Singh YD. Heavy metal priming plant stress tolerance deciphering through physiological, biochemical, molecular and omics mechanism. S Afr J Bot. 2024;168:16–25.
27. Teschke R. Aluminum, arsenic, beryllium, cadmium, chromium, cobalt, copper, iron, lead, mercury, molybdenum, nickel, platinum, thallium, titanium, vanadium, and zinc: molecular aspects in experimental liver injury. Int J Mol Sci. 2022;23(20):12213.
28. Abbas M, Li Y, Elbaiomy RG, Yan K, Ragauskas AJ, Yadav V, Soaud SA, Islam MM, Saleem N, Noor Z. Genome-wide analysis and expression profiling of SlHsp70 gene family in Solanum lycopersicum revealed higher expression of SlHsp70-11 in roots under Cd^{2+} stress. Front Biosci. 2022;27(6):186.
29. El-Sappah AH, Abbas M, Rather SA, Wani SH, Soaud N, Noor Z, Qiulan H, Eldomiaty AS, Mir RR, Li J. Genome-wide identification and expression analysis of metal tolerance protein (MTP) gene family in soybean (Glycine max) under heavy metal stress. Mol Biol Rep. 2023;50(4):2975–90.
30. Javed A, Iqbal T, Naseer H, Mumtaz AS, Younas A, Afsheen S, Alobaid AA, Warad I. Oxidative stress signatures and lipid accretion in Desmodesmus subspicatus under in vitro drought stress simulation. Biomass Convers Biorefin. 2024; doi: 10.1007/s13399-024-05624-z
31. Mansoor S, Mir MA, Karunathilake E, Rasool A, Ştefanescu DM, Chung YS, Sun H-J. Strigolactones as promising biomolecule for oxidative stress management: a comprehensive review. Plant Physiol Biochem. 2023;108282.
32. Ahmad R, Ali S, Abid M, Rizwan M, Ali B, Tanveer A, Ahmad I, Azam M, Ghani MA. Glycinebetaine alleviates the chromium toxicity in Brassica oleracea L. by suppressing oxidative stress and modulating the plant morphology and photosynthetic attributes. Environ Sci Pollut Res. 2020;27:1101–11.
33. Altaf MA, Hao Y, He C, Mumtaz MA, Shu H, Fu H, Wang Z. Physiological and biochemical responses of pepper (Capsicum annuum L.) seedlings to nickel toxicity. Front Plant Sci. 2022;13:950392.
34. Angulo-Bejarano PI, Puente-Rivera J, Cruz-Ortega R. Metal and metalloid toxicity in plants: an overview on molecular aspects. Plants. 2021;10(4):635.
35. Huihui Z, Xin L, Zisong X, Yue W, Zhiyuan T, Meijun A, Yuehui Z, Wenxu Z, Nan X, Guangyu S. Toxic effects of heavy metals pb and cd on mulberry (Morus alba L.) seedling leaves: photosynthetic function and reactive oxygen species (ROS) metabolism responses. Ecotoxicol Environ Saf. 2020;195:110469.
36. Jawad Hassan M, Ali Raza M, Ur Rehman S, Ansar M, Gitari H, Khan I, Wajid M, Ahmed M, Abbas Shah G, Peng Y. Effect of cadmium toxicity on growth, oxidative damage, antioxidant defense system and cadmium accumulation in two sorghum cultivars. Plants. 2020;9(11):1575.
37. Kumar S, Wang M, Liu Y, Fahad S, Qayyum A, Jadoon SA, Chen Y, Zhu G. Nickel toxicity alters growth patterns and induces oxidative stress response in sweetpotato. Front Plant Sci. 2022;13:1054924.
38. Rao MJ, Wu S, Duan M, Wang L. Antioxidant metabolites in primitive, wild, and cultivated citrus and their role in stress tolerance. Molecules. 2021;26(19):5801.
39. Ashraf MA, Riaz M, Arif MS, Rasheed R, Iqbal M, Hussain I, Mubarik MS. The role of non-enzymatic antioxidants in improving abiotic stress tolerance in plants. In: Hasanuzzaman M, Fujita M, Oku H, Islam MT, editors. Plant tolerance to environmental stress. CRC Press; 2019. pp. 129–44.
40. Garcia-Caparros P, De Filippis L, Gul A, Hasanuzzaman M, Ozturk M, Altay V, Lao MT. Oxidative stress and antioxidant metabolism under adverse environmental conditions: a review. Bot Rev. 2021;87:421–66.
41. Sachdev S, Ansari SA, Ansari MI, Fujita M, Hasanuzzaman M. Abiotic stress and reactive oxygen species: generation, signaling, and defense mechanisms. Antioxidants. 2021;10(2):277.
42. Kumar S, Yadav A, Verma R, Dubey AK, Narayan S, Pandey A, Sahu A, Srivastava S, Sanyal I. Metallothionein (MT1): a molecular stress marker in chickpea enhances drought and heavy metal stress adaptive efficacy in transgenic plants. Environ Exp Bot. 2022;199:104871.
43. Nykiel M, Gietler M, Fidler J, Prabucka B, Rybarczyk-Płońska A, Graska J, Boguszewska-Mańkowska D, Muszyńska E, Morkunas I, Labudda M. Signal transduction in cereal plants struggling with environmental stresses: from perception to response. Plants. 2022;11(8):1009.
44. Hwang E-W, Shin S-J, Park S-C, Jeong M-J, Kwon H-B. Identification of miR172 family members and their putative targets responding to drought stress in Solanum tuberosum. Genes Genomics. 2011;33:105–10.
45. Miskiewicz J, Tomczyk K, Mickiewicz A, Sarzynska J, Szachniuk M. Bioinformatics study of structural patterns in plant microRNA precursors. Biomed Res Int. 2017;2017(1):6783010.
46. Treiber T, Treiber N, Meister G. Regulation of microRNA biogenesis and its crosstalk with other cellular pathways. Nat Rev Mol Cell Biol. 2019;20(1):5–20.
47. Noman A, Aqeel M. miRNA-based heavy metal homeostasis and plant growth. Environ Sci Pollut Res. 2017;24:10068–82.
48. Sun X, Lin L, Sui N. Regulation mechanism of microRNA in plant response to abiotic stress and breeding. Mol Biol Rep. 2019;46:1447–57.
49. Pegler JL, Oultram JM, Nguyen DQ, Grof CP, Eamens AL. MicroRNA-mediated responses to cadmium stress in Arabidopsis thaliana. Plants. 2021;10(1):130.
50. Talukder P, Saha A, Roy S, Ghosh G, Roy DD, Barua S. Role of Mi RNA in phytoremediation of heavy metals and metal induced stress alleviation. Appl Biochem Biotechnol. 2023;195(9):5712–29.
51. Thornburg TE, Liu J, Li Q, Xue H, Wang G, Li L, Fontana JE, Davis KE, Liu W, Zhang B. Potassium deficiency significantly affected plant growth and development as well as microRNA-mediated mechanism in wheat (Triticum aestivum L). Front Plant Sci. 2020;11:1219.
52. Neysanian M, Iranbakhsh A, Ahmadvand R, Ardebili ZO, Ebadi M. Selenium nanoparticles conferred drought tolerance in tomato plants by altering the transcription pattern of microRNA-172 (miR-172), bZIP, and CRTISO genes,

upregulating the antioxidant system, and stimulating secondary metabolism. Protoplasma. 2024;261(4):735–47.
53. Reinhart BJ, Weinstein EG, Rhoades MW, Bartel B, Bartel DP. MicroRNAs in plants. Genes Dev. 2002;16(13):1616–26.
54. Ó'Maoiléidigh DS, van Driel AD, Singh A, Sang Q, Le Bec N, Vincent C, de Olalla EBG, Vayssières A, Romera Branchat M, Severing E. Systematic analyses of the MIR172 family members of Arabidopsis define their distinct roles in regulation of APETALA2 during floral transition. PLoS Biol. 2021;19(2):e3001043.
55. Luo Y, Guo Z, Li L. Evolutionary conservation of microRNA regulatory programs in plant flower development. Dev Biol. 2013;380(2):133–44.
56. Lian H, Wang L, Ma N, Zhou CM, Han L, Zhang TQ, Wang JW. Redundant and specific roles of individual MIR172 genes in plant development. PLoS Biol. 2021;19(2):e3001044.
57. Bansal C, Balyan S, Mathur S. Inferring the regulatory network of the miRNA-mediated response to individual and combined heat and drought stress in tomato. J Plant Biochem Biot. 2021;30:862–77.
58. Cheng X, He Q, Tang S, Wang H, Zhang X, Lv M, Liu H, Gao Q, Zhou Y, Wang Q. The miR172/IDS1 signaling module confers salt tolerance through maintaining ROS homeostasis in cereal crops. New Phytol. 2021;230(3):1017–33.
59. Swida-Barteczka A, Pacak A, Kruszka K, Nuc P, Karlowski WM, Jarmolowski A, Szweykowska-Kulinska Z. MicroRNA172b-5p/trehalose-6-phosphate synthase module stimulates trehalose synthesis and microRNA172b-3p/AP2-like module accelerates flowering in barley upon drought stress. Front Plant Sci. 2023;14:1124785.
60. Kang J, Singh H, Singh G, Kang H, Kalra VP, Kaur J. Abiotic stress and its amelioration in cereals and pulses: a review. Int J Curr Microbiol Appl Sci. 2017;6(3):1019–45.
61. Aslam M, Saeed MS, Sattar S, Sajad S, Sajjad M, Adnan M, Iqbal M, Sharif MT. Specific role of proline against heavy metals toxicity in plants. Int J Pure Appl Biosci. 2017;5(6):27–34.
62. Khatun J, Intekhab A, Dhak D. Effect of uncontrolled fertilization and heavy metal toxicity associated with arsenic (as), lead (pb) and cadmium (cd), and possible remediation. Toxicol. 2022;477:153274.
63. Rashid A, Schutte BJ, Ulery A, Deyholos MK, Sanogo S, Lehnhoff EA, Beck L. Heavy metal contamination in agricultural soil: environmental pollutants affecting crop health. Agron. 2023;13(6):1521.
64. Zulfiqar U, Haider FU, Ahmad M, Hussain S, Maqsood MF, Ishfaq M, Shahzad B, Waqas MM, Ali B, Tayyab MN. Chromium toxicity, speciation, and remediation strategies in soil-plant interface: a critical review. Front Plant Sci. 2023;13:1081624.
65. Azizi I, Esmaielpour B, Fatemi H. Exogenous nitric oxide on morphological, biochemical and antioxidant enzyme activity on savory (Satureja hortensis L.) plants under cadmium stress. J Saudi Soc Agric Sci. 2021;20(6):417–23.
66. Hafeez A, Rasheed R, Ashraf MA, Qureshi FF, Hussain I, Iqbal M. Effect of heavy metals on growth, physiological and biochemical responses of plants. In: Husen A, editor. Plants and their interaction to environmental pollution. Elsevier; 2023;139–59.
67. AbdElgawad H, Zinta G, Hamed BA, Selim S, Beemster G, Hozzein WN, Wadaan MA, Asard H, Abuelsoud W. Maize roots and shoots show distinct profiles of oxidative stress and antioxidant defense under heavy metal toxicity. Environ Pollut. 2020;258:113705.
68. Rizvi A, Khan M. Heavy metal-mediated toxicity to maize: oxidative damage, antioxidant defence response and metal distribution in plant organs. Int J Environ Sci Technol. 2019;16:4873–86.
69. Naz H, Naz A, Ashraf S. Impact of heavy metal toxicity to plant growth and nodulation in chickpea grown under heavy metal stress. Int J Res Emerg Sci Technol. 2015;2(5):248–60.
70. Adhikary A, Kumar R, Pandir R, Bhardwaj P, Wusirika R, Kumar S. Pseudomonas citronellolis; a multi-metal resistant and potential plant growth promoter against arsenic (V) stress in chickpea. Plant Physiol Biochem. 2019;142:179–92.
71. Ullah S, Khan J, Hayat K, Abdelfattah Elateeq A, Salam U, Yu B, Ma Y, Wang H, Tang Z-H. Comparative study of growth, cadmium accumulation and tolerance of three chickpea (Cicer arietinum L.) cultivars. Plants. 2020;9(3):310.
72. Ovečka M, Takáč T. Managing heavy metal toxicity stress in plants: biological and biotechnological tools. Biotechnol Adv. 2014;32(1):73–86.
73. Ghori N-H, Ghori T, Hayat M, Imadi S, Gul A, Altay V, Ozturk M. Heavy metal stress and responses in plants. Int J Environ Sci Technol. 2019;16:1807–28.
74. Gill M. Heavy metal stress in plants: a review. Int J Adv Res. 2014;2(6):1043–55.
75. Hossain MA, Piyatida P, da Silva JAT, Fujita M. Molecular mechanism of heavy metal toxicity and tolerance in plants: central role of glutathione in detoxification of reactive oxygen species and methylglyoxal and in heavy metal chelation. J Bot. 2012; 2012(1):872875.
76. Oteiza PI, Verstraeten SV. Interactions of Al and related metals with membrane phospholipids: consequences on membrane physical properties. Adv Planar Lipid Bilayers Liposomes. 2006;4:79–106.
77. Janicka-Russak M, Kabała K, Burzyński M, Kłobus G. Response of plasma membrane H+-ATPase to heavy metal stress in Cucumis sativu s roots. J Exp Bot. 2008;59(13):3721–8.
78. Abbas G, Murtaza B, Bibi I, Shahid M, Niazi NK, Khan MI, Amjad M, Hussain M. Natasha arsenic uptake, toxicity, detoxification, and speciation in plants: physiological, biochemical, and molecular aspects. Int J Environ Res Public Health. 2018;15(1):59.
79. Dias MC, Mariz-Ponte N, Santos C. Lead induces oxidative stress in Pisum sativum plants and changes the levels of phytohormones with antioxidant role. Plant Physiol Biochem. 2019;137:121–9.
80. Gopal R, Rizvi AH, Nautiyal N. Chromium alters iron nutrition and water relations of spinach. J Plant Nutr. 2009;32(9):1551–9.
81. Pandey N, Pathak G. Nickel alters antioxidative defense and water status in green gram. Indian J Plant Physiol. 2006;11(2):113.
82. Zouari M, Ahmed CB, Zorrig W, Elloumi N, Rabhi M, Delmail D, Rouina BB, Labrousse P, Abdallah FB. Exogenous proline mediates alleviation of cadmium stress by promoting photosynthetic activity, water status and antioxidative enzymes activities of young date palm (Phoenix dactylifera L). Ecotoxicol Environ Saf. 2016;128:100–8.
83. Roy RN, Saha B. Plants response to heavy metal stress. Stress physiology of Woody plants. In: Dai W, editor. Stress Physiology of Woody Plants. CRC Press; 2019. pp. 203–58.
84. Ameen N, Amjad M, Murtaza B, Abbas G, Shahid M, Imran M, Naeem MA, Niazi NK. Biogeochemical behavior of nickel under different abiotic stresses: toxicity and detoxification mechanisms in plants. Environ Sci Pollut Res. 2019;26:10496–514.
85. Bhalerao SA, Sharma AS, Poojari AC. Toxicity of nickel in plants. Int J Pure Appl Biosci. 2015;3(2):345–55.
86. Pietrini F, Iori V, Cheremisina A, Shevyakova NI, Radyukina N, Kuznetsov VV, Zacchini M. Evaluation of nickel tolerance in Amaranthus paniculatus L. plants by measuring photosynthesis, oxidative status, antioxidative response and metal-binding molecule content. Environ Sci Pollut Res. 2015;22:482–94.
87. Jagetiya B, Soni A, Yadav S. Effect of nickel on plant water relations and growth in green gram. Indian J Plant Physiol. 2013;18:372–6.
88. Vezza ME, Llanes A, Travaglia C, Agostini E, Talano MA. Arsenic stress effects on root water absorption in soybean plants: physiological and morphological aspects. Plant Physiol Biochem. 2018;123:8–17.
89. Zhang M, Duan L, Tian X, He Z, Li J, Wang B, Li Z. Uniconazole-induced tolerance of soybean to water deficit stress in relation to changes in photosynthesis, hormones and antioxidant system. J Plant Physiol. 2007;164(6):709–17.
90. Ma Y-L, Wang H-F, Wang P, Yu C-G, Luo S-Q, Zhang Y-F, Xie Y-F. Effects of cadmium stress on the antioxidant system and chlorophyll fluorescence characteristics of two Taxodium clones. Plant Cell Rep. 2018;37:1547–55.
91. Piotto FA, Carvalho MEA, Souza LA, Rabêlo FHS, Franco MR, Batagin-Piotto KD, Azevedo RA. Estimating tomato tolerance to heavy metal toxicity: cadmium as study case. Environ Sci Pollut Res. 2018;25:27535–44.
92. Giannakoula A, Therios I, Chatzissavvidis C. Effect of lead and copper on photosynthetic apparatus in citrus (Citrus aurantium L.) plants. The role of antioxidants in oxidative damage as a response to heavy metal stress. Plants. 2021;10(1):155.
93. Navabpour S, Yamchi A, Bagherikia S, Kafi H. Lead-induced oxidative stress and role of antioxidant defense in wheat (Triticum aestivum L). Physiol Mol Biol Plants. 2020;26:793–802.
94. Berni R, Luyckx M, Xu X, Legay S, Sergeant K, Hausman J-F, Lutts S, Cai G, Guerriero G. Reactive oxygen species and heavy metal stress in plants: impact on the cell wall and secondary metabolism. Environ Exp Bot. 2019;161:98–106.
95. Mahey S, Kumar R, Sharma M, Kumar V, Bhardwaj R. A critical review on toxicity of cobalt and its bioremediation strategies. SN Appl Sci. 2020;2(7):1279.
96. Bushra S, Faizan S. Oxidative stress and response of antioxidants during cadmium stress in chickpea (Cicer arietinum L.). Recent Res Agric Doubling Farmer's Income. 2019;50.
97. Kapoor RT, Hefft DI, Ahmad A. Nitric oxide and spermidine alleviate arsenic-incited oxidative damage in Cicer arietinum by modulating glyoxalase and antioxidant defense system. Funct Plant Biol. 2023;50(2):108-120
98. Vaishnani B, Nathwani SA, Baraiya T, Panigrahi J. Physiological, biochemical, and enzymatic implications of salt and lead tolerance in Cicer arietinum under hydroponic culture condition. Egypt J Agric Res. 2022;100(4):483–98.

99. Yadav R, Jain V, Hegde V, Yadav N, Kumar R. Bio-physico-chemical response of drought tolerant chickpeas to nickel. Legume Res. 2020;43(3):345–52.
100. Khatun S, Ali MB, Hahn E-J, Paek K-Y. Copper toxicity in Withania somnifera: growth and antioxidant enzymes responses of in vitro grown plants. Environ Exp Bot. 2008;64(3):279–85.
101. Jung H-i, Kong M-S, Lee B-R, Kim T-H, Chae M-J, Lee E-J, Jung G-B, Lee C-H, Sung J-K, Kim Y-H. Exogenous glutathione increases arsenic translocation into shoots and alleviates arsenic-induced oxidative stress by sustaining ascorbate–glutathione homeostasis in rice seedlings. Front Plant Sci. 2019;10:1089.
102. Wakeel A, Xu M, Gan Y. Chromium-induced reactive oxygen species accumulation by altering the enzymatic antioxidant system and associated cytotoxic, genotoxic, ultrastructural, and photosynthetic changes in plants. Int J Mol Sci. 2020;21(3):728.
103. Al-Sammarraie ON, Alsharafa KY, Al-Limoun MO, Khleifat KM, Al-Sarayreh SA, Al-Shuneigat JM, Kalaji HM. Effect of various abiotic stressors on some biochemical indices of Lepidium sativum plants. Sci Rep. 2020;10(1):21131.
104. Kumar D, Seth CS. Photosynthesis, lipid peroxidation, and antioxidative responses of Helianthus annuus L. against chromium (VI) accumulation. Int J Phytorem. 2022;24(6):590–9.
105. Hasanuzzaman M, Parvin K, Bardhan K, Nahar K, Anee TI, Masud AAC, Fotopoulos V. Biostimulants for the regulation of reactive oxygen species metabolism in plants under abiotic stress. Cells. 2021;10(10):2537.
106. Malecka A, Piechalak A, Mensinger A, Hanć A, Baralkiewicz D, Tomaszewska B. Antioxidative defense system in Pisum sativum roots exposed to heavy metals (pb, Cu, Cd, Zn). Pol J Environ Stud. 2012;21(6).
107. Altaf MA, Hao Y, Shu H, Mumtaz MA, Cheng S, Alyemeni MN, Ahmad P, Wang Z. Melatonin enhanced the heavy metal-stress tolerance of pepper by mitigating the oxidative damage and reducing the heavy metal accumulation. J Hazard Mater. 2023;454:131468.
108. Hammami H, Parsa M, Bayat H, Aminifard MH. The behavior of heavy metals in relation to their influence on the common bean (Phaseolus vulgaris) symbiosis. Environ Exp Bot. 2022;193:104670.
109. Qin S, Liu H, Nie Z, Gao W, Li C, Lin Y, Zhao P. AsA-GSH cycle and antioxidant enzymes play important roles in cd tolerance of wheat. Bull Environ Contam Toxicol. 2018;101(5):684–90.
110. Shah AA, Shah AN, Bilal Tahir M, Abbas A, Javad S, Ali S, Rizwan M, Alotaibi SS, Kalaji HM, Telesinski A, et al. Harzianopyridone Supplementation reduced chromium uptake and enhanced activity of antioxidant enzymes in Vigna radiata seedlings exposed to chromium toxicity. Front Plant Sci. 2022;13:881561.
111. Sirhindi G, Mir MA, Abd-Allah EF, Ahmad P, Gucel S. Jasmonic acid modulates the physio-biochemical attributes, antioxidant enzyme activity, and gene expression in Glycine max under nickel toxicity. Front Plant Sci. 2016;7:591.
112. Thakur S, Singh L, Zularisam A, Sakinah M, Din M. Lead induced oxidative stress and alteration in the activities of antioxidative enzymes in rice shoots. Biol Plant. 2017;61:595–8.
113. Tang CF, Liu YG, Zeng GM, Li X, Xu WH, Li CF, Yuan XZ. Effects of exogenous spermidine on antioxidant system responses of Typha latifolia L. under Cd2 + stress. J Integr Plant Biol. 2005;47(4):428–34.
114. Ifeanyi OE. A review on free radicals and antioxidants. Int J Curr Res Med Sci. 2018;4(2):123–33.
115. Hadwan MH, Hussein MJ, Mohammed RM, Hadwan AM, Saad Al-Kawaz H, Al-Obaidy SS, Al Talebi ZA. An improved method for measuring catalase activity in biological samples. Biol Methods Protoc. 2024;9(1):bpae015.
116. Gharib FAEL, Ahmed EZ. Spirulina platensis improves growth, oil content, and antioxidant activitiy of rosemary plant under cadmium and lead stress. Sci Rep. 2023;13(1):8008.
117. Hasanuzzaman M, Raihan MRH, Siddika A, Rahman K, Nahar K. Supplementation with Ascophyllum nodosum extracts mitigates arsenic toxicity by modulating reactive oxygen species metabolism and reducing oxidative stress in rice. Ecotoxicol Environ Saf. 2023;255:114819.
118. Rizwan M, Nawaz A, Irshad S, Manoharadas S. Exogenously applied melatonin enhanced chromium tolerance in pepper by up-regulating the photosynthetic apparatus and antioxidant machinery. Sci Hortic. 2024;323:112468.
119. Spormann S, Soares C, Martins V, Azenha M, Gerós H, Fidalgo F. Early activation of antioxidant responses in Ni-stressed tomato cultivars determines their resilience under co-exposure to drought. J Plant Growth Regul. 2023;42(2):877–91.
120. Jiang B, Su C, Wang Y, Xu X, Li Y, Ma D. Genome-wide identification of glutathione peroxidase (GPX) family genes and silencing TaGPX3. 2A reduced disease resistance in wheat. Plant Physiol Biochem. 2023;204:108139.
121. Yang S, Chen X, Hui W, Ren Y, Ma L. Progress in responses of antioxidant enzyme systems in plant to environmental stresses. J Fujian Agric Forestry Univ (Natural Sci Edition). 2016;45(05):482–9.
122. Kang Y, Yao Y, Liu Y, Shi M, Zhang W, Zhang R, Li H, Qin S, Yang X. Exogenous glutathione enhances tolerance of the potato (Solanum tuberosum L.) to cadmium stress by regulating the biosynthesis of phenylpropanoid and the signal transduction of plant hormones. Chem Biol Technol Agric. 2023;10(1):24.
123. Natasha, Shahid M, Khalid S, Bibi I, Khalid S, Masood N, Qaisrani SA, Niazi NK, Dumat C. Arsenic-induced oxidative stress in Brassica oleracea: Multivariate and literature data analyses of physiological parameters, applied levels and plant organ type. Environ Geochem Health. 2022:1–13.
124. Solórzano E, Corpas FJ, González-Gordo S, Palma JM. Reactive oxygen species (ROS) metabolism and nitric oxide (NO) content in roots and shoots of rice (Oryza sativa L.) plants under arsenic-induced stress. Agron. 2020;10(7):1014.
125. Ibrahim M, Nawaz S, Iqbal K, Rehman S, Ullah R, Nawaz G, Almeer R, Sayed AA, Peluso I. Plant-derived smoke solution alleviates cellular oxidative stress caused by arsenic and mercury by modulating the cellular antioxidative defense system in wheat. Plants. 2022;11(10):1379.
126. Bagherzadeh Homaee M, Ehsanpour AA. Silver nanoparticles and silver ions: oxidative stress responses and toxicity in potato (Solanum tuberosum L.) grown in vitro. Hortic Environ Biote. 2016;57:544–53.
127. Bhagyawant SS, Narvekar DT, Gupta N, Bhadkaria A, Koul KK, Srivastava N. Variations in the antioxidant and free radical scavenging under induced heavy metal stress expressed as proline content in chickpea. Physiol Mol Biol Plants. 2019;25:683–96.
128. Kumar A, Dubey AK, Kumar V, Ansari MA, Narayan S, Kumar S, Pandey V, Shirke PA, Pande V, Sanyal I. Over-expression of chickpea glutaredoxin (CaGrx) provides tolerance to heavy metals by reducing metal accumulation and improved physiological and antioxidant defence system. Ecotoxicol Environ Saf. 2020;192:110252.
129. Tousi S, Zoufan P, Ghahfarrokhie AR. Alleviation of cadmium-induced phytotoxicity and growth improvement by exogenous melatonin pretreatment in mallow (Malva parviflora) plants. Ecotoxicol Environ Saf. 2020;206:111403.
130. Kalai T, Khamassi K, Teixeira da Silva JA, Gouia H, Bettaieb Ben-Kaab L. Cadmium and copper stress affect seedling growth and enzymatic activities in germinating barley seeds. Arch Agron Soil Sci. 2014;60(6):765–83.
131. Bushra S, Faizan S, Mushtaq Z, Hussain A, Hakeem KR. Effect of cadmium stress on the growth, physiology, stress markers, antioxidants and stomatal behaviour of two genotypes of chickpea (Cicer arietinum L.). 2022;1(9):1987-2004
132. Joudah MT, Ramadi A-I. Action of lead and cadmium stress on inhibitor's activity in Germinated seedlings of Chickpea Plant. Plant Arch. 2021;21(1):611–6.
133. Rakkammal K, Pandian S, Ramesh M. Physiological and biochemical response of finger millet plants exposed to arsenic and nickel stress. Plant Stress. 2024;11:100389.
134. Badiaa O, Yssaad HAR, Topcuoglu B. Effect of heavy metals (copper and zinc) on proline, polyphenols and flavonoids content of tomato (Lycopersicon esculentum Mill). Plant Arch. (09725210). 2020;20(2).
135. Arbona V, Manzi M, Zandalinas SI, Vives-Peris V, Pérez-Clemente RM, Gómez-Cadenas A. Physiological, metabolic, and molecular responses of plants to abiotic stress. Stress Signal Plants Genomics Proteom Perspective. 2017;2:1–35.
136. Kaur G, Jain S, Bhushan S, Das N, Sharma M, Sharma D. Role of microRNAs and their putative mechanism in regulating potato (Solanum tuberosum L.) life cycle and response to various environmental stresses. Plant Physiol Biochem. 2024;27:108334.
137. Sharma P, Kumar A, Bhardwaj R. Plant steroidal hormone epibrassinolide regulate–heavy metal stress tolerance in Oryza sativa L. by modulating antioxidant defense expression. Environ Exp Bot. 2016;122:1–9.
138. Alwutayd KM, Alghanem SMS, Alwutayd R, Alghamdi SA, Alabdallah NM, Al-Qthanin RN, Sarfraz W, Khalid N, Naeem N, Ali B. Mitigating chromium toxicity in rice (Oryza sativa L.) via ABA and 6-BAP: unveiling synergistic benefits on morphophysiological traits and ASA-GSH cycle. Sci Total Environ. 2024;908:168208.
139. Chen M, Jiang P, Zhang X, Sunahara GI, Liu J, Yu G. Physiological and biochemical responses of Leersia hexandra Swartz to nickel stress: insights into antioxidant defense mechanisms and metal detoxification strategies. J Hazard Mater. 2024;466:133578.
140. Hussain I, Ashraf MA, Rasheed R, Iqbal M, Ibrahim M, Zahid T, Thind S, Saeed F. Cadmium-induced perturbations in growth, oxidative defense

system, catalase gene expression and fruit quality in tomato. Int J Agric Biol. 2017;19(1).
141. Kumar A, Singh RP, Singh PK, Awasthi S, Chakrabarty D, Trivedi PK, Tripathi RD. Selenium ameliorates arsenic induced oxidative stress through modulation of antioxidant enzymes and thiols in rice (Oryza sativa L). Ecotoxicol. 2014;23:1153–63.
142. Khandal H, Parween S, Roy R, Meena MK, Chattopadhyay D. MicroRNA profiling provides insights into post-transcriptional regulation of gene expression in chickpea root apex under salinity and water deficiency. Sci Rep. 2017;7(1):4632.
143. Chen C, Ridzon DA, Broomer AJ, Zhou Z, Lee DH, Nguyen JT, Barbisin M, Xu NL, Mahuvakar VR, Andersen MR. Real-time quantification of microRNAs by stem–loop RT–PCR. Nucleic Acids Res. 2005;33(20):e179–179.
144. Jung HJ, Kang H. Expression and functional analyses of microRNA417 in Arabidopsis thaliana under stress conditions. Plant Physiol Biochem. 2007;45(10–11):805–11.
145. Li Y, Li W, JIN YX. Computational identification of novel family members of microRNA genes in Arabidopsis thaliana and Oryza sativa. Acta Biochim Biophys Sin. 2005;37(2):75–87.
146. Zhu Q-H, Upadhyaya NM, Gubler F, Helliwell CA. Over-expression of miR172 causes loss of spikelet determinacy and floral organ abnormalities in rice (Oryza sativa). BMC Plant Biol. 2009;9:1–13.
147. Tripathi RK, Bregitzer P, Singh J. Genome-wide analysis of the SPL/miR156 module and its interaction with the AP2/miR172 unit in barley. Sci Rep. 2018;8(1):7085.
148. Lee S, Singh MB, Bhalla PL. Functional analysis of soybean miR156 and miR172 in tobacco highlights their role in plant morphology and floral transition. Plant Physiol Biochem. 2023;196:393–401.
149. Bologna NG, Mateos JL, Bresso EG, Palatnik JF. A loop-to-base processing mechanism underlies the biogenesis of plant microRNAs miR319 and miR159. EMBO J. 2009;28(23):3646–56.
150. Mateos JL, Bologna NG, Chorostecki U, Palatnik JF. Identification of microRNA processing determinants by random mutagenesis of Arabidopsis MIR172a precursor. Curr Biol. 2010;20(1):49–54.
151. Song L, Axtell MJ, Fedoroff NV. RNA secondary structural determinants of miRNA precursor processing in Arabidopsis. Curr Biol. 2010;20(1):37–41.
152. Mehrpooyan F, Othman R, Harikrishna J. Tissue and temporal expression of miR172 paralogs and the AP2-like target in oil palm (Elaeis guineensis Jacq). Tree Genet Genomes. 2012;8:1331–43.
153. Wang T, Ping X, Cao Y, Jian H, Gao Y, Wang J, Tan Y, Xu X, Lu K, Li J. Genome-wide exploration and characterization of miR172/euAP2 genes in Brassica napus L. for likely role in flower organ development. BMC Plant Biol. 2019;19:1–15.
154. Bansal C, Kumar A, Shrivastava M, Mathur S. Functional diversification of miR172 isoforms in tomato under abiotic stress. Environ Exp Bot. 2024;220:105696.
155. Ritika A, Namrata D, Rita S, Aman J. Genome-wide evolutionary analysis of precursor sequences of MIR156 and MIR172 family members in Brassica species. Res J Biotechnol. 2021;16:4.
156. Dash PK, Gupta P, Sreevathsa R, Pradhan SK, Sanjay TD, Mohanty MR, Roul PK, Singh NK, Rai R. Phylogenomic analysis of micro-RNA involved in juvenile to flowering-stage transition in photophilic rice and its sister species. Cells. 2023;12(10):1370.
157. Guo Z, Kuang Z, Deng Y, Li L, Yang X. Identification of species-specific microRNAs provides insights into dynamic evolution of microRNAs in plants. Int J Mol Sci. 2022;23(22):14273.
158. Moradi K, Khalili F. Assessment of pattern expression of miR172 and miR169 in response to drought stress in Echinacea purpurea L. Biocatal Agric Biotechnol. 2018;16:507–12.
159. Singroha G, Sharma P, Sunkur R. Current status of microRNA-mediated regulation of drought stress responses in cereals. Physiol Plant. 2021;172(3):1808–21.
160. Liu L, Yin H, Liu Y, Shen L, Yang X, Zhang D, Li M, Yan M. Analysis of cadmium-stress-induced microRNAs and their targets reveals bra-miR172b-3p as a potential Cd2+-specific resistance factor in Brassica juncea. Processes. 2021;9(7):1099.
161. Min Yang Z, Chen J. A potential role of microRNAs in plant response to metal toxicity. Metallomics. 2013;5(9):1184–90.
162. Liang G, Yang F, Yu D. MicroRNA395 mediates regulation of sulfate accumulation and allocation in Arabidopsis thaliana. Plant J. 2010;62(6):1046–57.
163. Srivastava S, Suprasanna P. MicroRNAs: tiny, powerful players of metal stress responses in plants. Plant Physiol Biochem. 2021;166:928–38.
164. Bhat A, Mishra S, Kaul S, Dhar MK. Comparative analysis of miRNA expression profiles in flowering and non-flowering tissue of Crocus sativus L. Protoplasma. 2024; 261(4):749-769.
165. Peng W, Song N, Li W, Yan M, Huang C, Yang Y, Duan K, Dai L, Wang B. Integrated analysis of MicroRNA and target genes in brachypodium distachyon infected by magnaporthe oryzae by small RNA and degradome sequencing. Front Plant Sci. 2021;12:742347.
166. Sharma R, Upadhyay S, Bhat B, Singh G, Bhattacharya S, Singh A. Abiotic stress induced miRNA-TF-gene regulatory network: a structural perspective. Genom. 2020;112(1):412–22.
167. Bukhari SAH, Shang S, Zhang M, Zheng W, Zhang G, Wang TZ, Shamsi IH, Wu F. Genome-wide identification of chromium stress-responsive micro RNAs and their target genes in tobacco (Nicotiana tabacum) roots. Environ Toxicol Chem. 2015;34(11):2573–82.
168. Jamla M, Patil S, Joshi S, Khare T, Kumar V. MicroRNAs and their exploration for developing heavy metal-tolerant plants. J Plant Growth Regul. 2022; 41:2579–2595
169. Yu Lj L, Yf, Liao B, Xie Lj, Chen L, Xiao S, Li J, Sn H. Shu Ws. Comparative transcriptome analysis of transporters, phytohormone and lipid metabolism pathways in response to arsenic stress in rice (Oryza sativa). New Phytol. 2012;195(1):97–112.
170. Ghosh S, Adhikari S, Adhikari A, Hossain Z. Contribution of plant miRNAome studies towards understanding heavy metal stress responses: current status and future perspectives. Environ Exp Bot. 2022;194:104705.
171. Li T-Z, Zheng Y-Z, Rong Y-Q, Wei S-L, Wang X-H, Tu P-F. Gene cloning, subcellular localization and expression analysis of the AsERF1 gene from Aquilaria sinensis. Yaoxue Xuebao. 2020;55(8):1957–64.
172. Inal B, Muslu S, Yigider E, Kasapoglu A, Ilhan E, Ciltas A, Yildirim E, Aydin M. In silico analysis of Phaseolus vulgaris L. metalloprotease FtsH gene: characterization and expression in drought and salt stress. Genet Resour Crop Evol. 2024; doi:10.1007/s10722-024-02031-1
173. He Q, Zhu S, Zhang B. MicroRNA–target gene responses to lead-induced stress in cotton (Gossypium hirsutum L). Funct Integr Genomics. 2014;14:507–15.
174. Çelik Ö, Akdaş EY. Tissue-specific transcriptional regulation of seven heavy metal stress-responsive miRNAs and their putative targets in nickel indicator castor bean (R. communis L.) plants. Ecotoxicol Environ Saf. 2019;170:682–90.
175. Ahammed GJ, Li CX, Li X, Liu A, Chen S, Zhou J. Overexpression of tomato RING E3 ubiquitin ligase gene SlRING1 confers cadmium tolerance by attenuating cadmium accumulation and oxidative stress. Physiol Plant. 2021;173(1):449–59.
176. Zhou ZS, Song JB, Yang ZM. Genome-wide identification of Brassica napus microRNAs and their targets in response to cadmium. J Exp Bot. 2012;63(12):4597–613.
177. Kang X, Gao J, Zhao J, Yin H, Wang W, Zhang P, Wang R, Xu J. Identification of cadmium-responsive microRNAs in Solanum torvum by high-throughput sequencing. Russ J Plant Physl. 2017;64:283–300.
178. Hoagland DR, Arnon DI. The water-culture method for growing plants without soil; 1938.
179. Lutts S, Kinet J, Bouharmont J. NaCl-induced senescence in leaves of rice (Oryza sativaL.) Cultivars differing in salinity resistance. Ann Bot. 1996;78(3):389–98.
180. Barrs H, Weatherley P. A re-examination of the relative turgidity technique for estimating water deficits in leaves. Aust J Biol Sci. 1962;15(3):413–28.
181. Gutiérrez-Rodríguez M, Reynolds MP, Escalante-Estrada JA, Rodríguez-González MT. Association between canopy reflectance indices and yield and physiological traits in bread wheat under drought and well-irrigated conditions. Aust J Agric Res. 2004;55(11):1139–47.
182. Shah SH, Houborg R, McCabe MF. Response of chlorophyll, carotenoid and SPAD-502 measurement to salinity and nutrient stress in wheat (*Triticum aestivum L*). Agron. 2017;7(3):61.
183. Shams M, Yildirim E, Ekinci M, Turan M, Dursun A, Parlakova F, Kul R. Exogenously applied glycine betaine regulates some chemical characteristics and antioxidative defence systems in lettuce under salt stress. Hortic Environ Biote. 2016;57:225–31.
184. Singh P, Kumar V, Sharma J, Saini S, Sharma P, Kumar S, Sinhmar Y, Kumar D, Sharma A. Silicon supplementation alleviates the salinity stress in wheat plants by enhancing the plant water status, photosynthetic pigments, proline content and antioxidant enzyme activities. Plants. 2022;11(19):2525.
185. Xiang D-B, Peng L-X, Zhao J-L, Zou L, Zhao G, Song C. Effect of drought stress on yield, chlorophyll contents and photosynthesis in tartary buckwheat (Fagopyrum tataricum). J Food Agric Environ. 2013;11:1358–63.

186. Chen C, Li J, Feng J, Liu B, Feng L, Yu X, Li G, Zhai J, Meyers BC, Xia R. sRNAanno—a database repository of uniformly annotated small RNAs in plants. Hortic Res. 2021;8.
187. Guo Z, Kuang Z, Zhao Y, Deng Y, He H, Wan M, Tao Y, Wang D, Wei J, Li L. PmiREN2. 0: from data annotation to functional exploration of plant microRNAs. Nucleic Acids Res. 2022;50(D1):D1475–82.
188. Goodstein DM, Shu S, Howson R, Neupane R, Hayes RD, Fazo J, Mitros T, Dirks W, Hellsten U, Putnam N. Phytozome: a comparative platform for green plant genomics. Nucleic Acids Res. 2012;40(D1):D1178–86.
189. Chao J, Li Z, Sun Y, Aluko OO, Wu X, Wang Q, Liu G. MG2C: a user-friendly online tool for drawing genetic maps. Mol Hortic. 2021;1:1–4.
190. Lorenz R, Bernhart SH, Höner zu Siederdissen C, Tafer H, Flamm C, Stadler PF, Hofacker IL. ViennaRNA Package 2.0. Algorithms Mol Biol. 2011;6:1–14.
191. Chen C, Wu Y, Li J, Wang X, Zeng Z, Xu J, Liu Y, Feng J, Chen H, He Y. TBtools-II: a one for all, all for one bioinformatics platform for biological big-data mining. Mol Plant. 2023;16(11):1733–42.
192. Thompson JD, Gibson TJ, Plewniak F, Jeanmougin F, Higgins DG. The CLUSTAL_X windows interface: flexible strategies for multiple sequence alignment aided by quality analysis tools. Nucleic Acids Res. 1997;25(24):4876–82.
193. Tamura K, Stecher G, Kumar S. MEGA11: molecular evolutionary genetics analysis version 11. Mol Biol Evol. 2021;38(7):3022–7.
194. He Z, Zhang H, Gao S, Lercher MJ, Chen W-H, Hu S. Evolview v2: an online visualization and management tool for customized and annotated phylogenetic trees. Nucleic Acids Res. 2016;44(W1):W236–41.
195. Dai X, Zhao PX. psRNATarget: a plant small RNA target analysis server. Nucleic Acids Res. 2011;39(suppl2):W155–9.
196. Jyothi M, Usha S, Suchithra B, Ulfath TS, Devaraj V, Babu RN. Boron toxicity induces altered expression of miRNAs in French bean (Phaseolus vulgaris L). J Appl Biol Biotechnol. 2018;6:1–10.
197. Qureshi R, Sacan A. A novel method for the normalization of microRNA RT-PCR data. BMC Med Genet. 2013;6:1–13.
198. Livak KJ, Schmittgen TD. Analysis of relative gene expression data using real-time quantitative PCR and the 2 – ΔΔCT method. Methods. 2001;25(4):402–8.

Publisher's note